The role of p53 and p21 in cell density dependent cisplatin resistance in ovarian cancer cells

by

Maya Anani

A Dissertation Submitted to the
Graduate School of Health Sciences
in Partial Fulfillment of the Requirements for
the Degree of

Master of Science

In

Cellular and Molecular Medicine

KOÇ
ÜNİVERSİTESİ

June 27th, 2025

The role of p53 and p21 in cell density dependent cisplatin resistance in ovarian cancer cells.

Koç University

Graduate School of Health Sciences

This is to certify that I have examined this copy of a master's thesis by

Maya Anani

and have found that it is complete and satisfactory in all respects,
and that any and all revisions required by the final
examining committee have been made.

Committee Members:

Assoc. Prof. Gülnihal Özcan (Thesis Advisor)

Prof. Dr. Murat Acar

Assist. Prof. Esma Nur Zeydanlı

Date: June 27th, 2025

Dedication

To my father, mother, and sister who filled my life with unwavering love, endless support and boundless sacrifices. The person I am today is only because of your continuous belief in my potential. Baba and Mama, you have and always will be my role models, I carry the values you installed in me every day. Your career achievements have always inspired me to become a hardworking person, aiming to follow in your footsteps.

This thesis is as much yours as it is mine.

ABSTRACT

The role of p53 and p21 in cell density dependent cisplatin resistance in ovarian cancer cells

Maya Anani

Master of Science in Cellular and Molecular Medicine

June 27th, 2025

Chemoresistance is one of the major challenges in ovarian cancer. Resistant cancer cells which lead to disease relapse are the most prominent causes of death in ovarian cancer patents. Cisplatin is one of the most common platinum-based chemotherapeutic agents used to treat ovarian cancer. It's main mechanism of action involves inhibiting transcription by covalently binding to DNA, forming adducts which cause DNA damage and resulting in cell death. Tumor suppressor p53 exhibits great importance in determining whether the cells will go into apoptosis or repair DNA damage upon exposure to cisplatin. Associated with p53 is p21, a cyclin dependent kinase inhibitor (CDK) that is directly responsible for cell cycle arrest and cellular repair at the G1/S and G2/ phases of the cell cycle. Despite that the use of cisplatin increased effectiveness of chemotherapy in ovarian cancer, resistance to cisplatin is a major handicap in the clinic.

Recent studies have suggested a new mode of cisplatin resistance in ovarian cancer cells, which is cell density-dependent cisplatin resistance at which ovarian cancer cells exhibit increased resistance to cisplatin as the cell density in cancer cell populations increase. Although cell density-dependent cisplatin resistance may have important clinical implications, its underlying mechanisms are not clear.

To understand how cellular density affects cisplatin resistance in ovarian cancer, in this thesis we investigated the responses of sensitive (A2780) and resistant (CP16) ovarian cancer cell lines to cisplatin at low, confluent, and overconfluent culture conditions. In order to evaluate the contribution of p53 and p21's functions in cell density dependent chemoresistance we assessed the differential protein expression of p53 and p21 along with their phosphorylated forms at different subcellular fractions. Hence, we aimed to shed light on possible mechanisms of cisplatin resistance at increasing confluence levels. Moreover, we investigated the changes in the influx and efflux pumps that determine intracellular cisplatin accumulation to understand whether the degree of cell – cell interaction at different confluency levels affects the cells' cisplatin uptake or efflux capabilities.

Our study suggests that p53 and p21 are regulated in a cell density dependent manner in response to cisplatin, including changes in their phosphorylation and subcellular localization. In CP16 cells, the confluence dependent pattern of p53 and p21 regulation seem to support cisplatin resistance at higher cell densities, while in A2780, the opposite pattern is observed.

ÖZETÇE
Over Kanseri Hücrelerinde Hücre Yoğunluğu Bağımlı Sisplatin Direncinde p53 ve p21'in Rolü

Maya Anani
Hücresel ve Moleküler Tıp Yüksek Lisans Tezi
13 Haziran 202

Kemorezistans, over (yumurtalık) kanserinde karşılaşılan en büyük zorluklardan biridir. Hastalığın nüksüne neden olan dirençli kanser hücreleri, over kanseri hastalarında en yaygın ölüm nedenleri arasında yer almaktadır. Sisplatin, over kanserinin tedavisinde en yaygın kullanılan platin bazlı kemoterapötik ajanlardan biridir. Ana etki mekanizması, DNA'ya kovalent olarak bağlanarak adductlar (bağlantılar) oluşturması, bu yolla DNA hasarına neden olması ve transkripsiyonu engelleyerek hücre ölümüne yol açmasıdır. Tümör baskılayıcı p53, hücrelerin sisplatin maruziyeti sonrası apoptoza mı gideceği yoksa DNA hasarını mı onaracağı kararında önemli bir rol oynar. p53 ile ilişkili olarak görev yapan p21, hücre döngüsünü G1/S ve G2/M evrelerinde durdurarak hücresel onarımdan sorumlu olan bir siklin-bağımlı kinaz inhibitörüdür (CDK inhibitörü). Sisplatinin kullanımı over kanserinde kemoterapinin etkinliğini arttırsa da, sisplatine direnç klinikte önemli bir zorluktur.

Son zamanlarda yapılan çalışmalar, over kanseri hücrelerinde yeni bir sisplatin direnç tipi tanımlamıştır. Hücre yoğunluğuna bağlı sisplatin direnci olarak tanımlanan bu direnç tipinde, kanser hücre popülasyonunda hücrelerin yoğunlukları arttıkça, sisplatine direnç artmaktadır. Bu direnç tipi önemli klinik sonuçları olabilecek bir direnç tipi olsa da, hücre yoğunluğu bağımlı sisplatin direncinin altında yatan mekanizmalar henüz net olarak bilinmemektedir.

Over kanserinde hücre yoğunluğunun sisplatin direncini nasıl etkilediğini anlayabilmek için, bu tez çalışmasında sisplatine duyarlı (A2780) ve dirençli (CP16) over kanseri hücre hatlarının sisplatine verdikleri yanıtlar, düşük, tam ve aşırı konfluent hücre kültürü koşullarında incelenmiştir. p53 ve p21'in hücre yoğunluğuna bağımlı kemorezistans üzerindeki katkılarını anlayabilmek amacıyla, bu proteinlerin ve fosforile formlarının farklı hücre alt fraksiyonlarındaki ekspresyon seviyeleri analiz edilmiştir. Bu şekilde, artan hücre yoğunluğu seviyelerinde sisplatin direncinin olası mekanizmalarını aydınlatmak hedeflenmiştir. Ayrıca, farklı yoğunluk seviyelerindeki hücre – hücre etkileşim derecesinin hücrelerin sisplatin alımı veya atılım kapasitelerini etkileyip etkilemediğini anlamak için hücre içi sisplatin birikimini belirleyen içeri alım ya da dışa atım pompalarındaki değişiklikler de incelenmiştir.

Çalışmamız, p53 ve p21'in sisplatine yanıt olarak hücre yoğunluğuna bağlı şekilde düzenlendiğini; bu bağlamda fosforilasyon durumlarında ve hücresel lokalizasyonlarında değişiklikler olduğunu göstermektedir. CP16 hücrelerinde gözlemlenen hücre yoğunluğu bağımlı p53 ve p21 düzenlenme paterni, yüksek hücre yoğunluğunda gözlenen sisplatin direncini açıklarken; A2780 hücrelerinde bunun tersi bir patern görülmektedir.

AKNOWLEDGEMENTS

First and foremost, I would like to extend my heartfelt gratitude to my supervisor, Associate Professor Gülnihal Özcan, for giving me the opportunity to peruse this research project and for her continuous guidance throughout the course of this degree. Throughout all obstacles, she showed me unwavering support and mentorship which I will always value. It has been a genuine joy to be her student.

I extend my heartfelt gratitude to Distinguished Professor Zahid Siddik from MD Anderson Cancer Center, who shared his valuable knowledge and experience to excel the ideas in this project. He opened his lab and resources for the conduction of this project. I want to also thank Guangan He from MD Anderson Cancer Center for his endless support for the execution of the study efficiently at the Siddik Lab.

I am grateful to Özen Leylek, Ph.D. and Assist. Prof. Gülin Özcan for their diligent work to optimize the techniques and establish the preliminary data that made the foundations for this study.

I would like to thank the Koç University Research Center for Translational Medicine for their research infrastructure, valuable support for laboratory utilities/services and endless support from all staff which made the research process efficient and delightful. I want to extend my gratitude to Koç University Visiting Scholar Program which supported Dr. Gülnihal Özcan's visits to MD Anderson Cancer Center and collaboration with Siddik Lab.

I want to thank my thesis committee members, Prof. Dr. Murat Acar and Assist. Prof. Esma Nur Zeydanlı for their valuable support and contribution in the advancements of this study.

I am grateful to laboratory members of KUTTAM, Bilge Abacar, Aminesena Baser, Rana Hanafi, and Ece Özmen for creating a warm, collaborative and welcoming working environment. I am especially thankful for Tevriz Dilan Demir, Ph.D. who took her time to teach me essential laboratory techniques, familiarizing with me the

laboratory environment and guiding me on the conduction of key methods in this study. Their companionship has been a powerful source of motivation.

I would like to thank my cousin Yazan Hamzeh, who introduced me to this field, sparked my interest in it and inspired me to follow this academic path.

Lastly, I owe my biggest appreciation to my father, Fadi Anani, my mother, Safa'a Masoud, and my sister, Meera Anani for their continuous support, understanding and encouragement throughout my academic path. In my moments of self-doubt and upon facing any obstacle, their belief gave me the strength to push forward. Being part of this family is a blessing that I thank Allah for every day.

Table of Contents

LIST OF TABLES

LIST OF FIGURES

ABBREVIATIONS

ATM	Ataxia-Telangiectasia Mutated
ATP7A	ATPase copper-transporting Alpha
ATP7B	ATPase copper-transporting Beta
ATR	Ataxia Telangiectasia and Rad3-related
BER	Base Excision Repair
BRCA1	Breast Cancer Type 1
BRCA2	Breast Cancer Type
CDKs	Cyclin Dependent Kinases
Chk1	Checkpoint Kinase 1
Chk2	Checkpoint Kinase 2
CK2	Casein Kinase 2
CTR1	Copper Transporter 1
DNA-PK	DNA-Protein Kinase
ERCC1	Excision Repair Cross-Complementation Group 1
GADD45a	Growth Arrest and DNA Damage-inducible 45 alpha
GSH	Glutathione
Her2-neu	Receptor Tyrosine-Protein Kinase erbB-2
MDM2	Mouse Double Minute 2 Homolog
MMR	Mismatch Repair
NHEJ	Non-Homologous End Joining
p21	Protein 21
p53	Protein 53
PCNA	Proliferating Cell Nuclear Antigen
PI3K/Akt	Phosphatidylinositol 3-Kinase/Protein Kinase B
PIN1	Peptidyl-prolyl cis/trans isomerase 1
PKA	Protein Kinase A
PRPK	p53-related protein kinase
PTM	Post Translational Modification
TGF-β	Transforming Growth Factor β
TLS	Translesion DNA Synthesis
XIAP	X Inhibitor of Apoptosis Protein
XPA/F	Xeroderma Pigmentosum Complementation Group A/F

Chapter 1:
INTRODUCTION

1.1 Ovarian Cancer

Ovarian cancer is the deadliest type of gynecological cancer in women, originating primarily in the ovarian tissue. Not only does ovarian cancer rank as the 8th most common leading cause of death but it is also considered to be the 7th most occurring cancer in women worldwide as of 2023 (Coalition, 2023). The high mortality rate is due to the difficulty in diagnosing the disease at an early stage. Women aged 55-64 years old are the most common population diagnosed with ovarian cancer; however, it can still occur at any age. The most commonly diagnosed type that amounts to 90% of cases is epithelial ovarian cancer. Other less commonly diagnosed types of ovarian cancer include sex cord stromal, germ cell, and mixed cell type. Despite advancements in research and treatment, the survival rate of ovarian cancer patients is much lower in comparison to other cancers, estimating a 5- year survival rate of 50% (ESMO, 2017)

Diagnosing ovarian cancer at an early stage continues to be a challenge due to non-specific symptoms such as bloating, frequent need to urinate, and pelvic or abdominal pain. Despite the ongoing challenge in diagnosis, risk factors such as family history, multiple pregnancies, obesity, early menstruation/late menopause, and BRCA1 or BRCA2 mutations play an important role in screening the disease for early detection. One of the most important risk factors is the BRCA1 or BRCA2 mutation. According to ESMO, inheriting the BRCA1 mutation increases the risk of developing ovarian cancer by 15-45% while inheriting the BRCA2 increases the risk by 10-20%. Therefore, women with either BRCA1 or BRCA2 mutations are advised to surgically remove their ovaries and fallopian tubes before reaching the age of 40. Additionally, women within the age group that express increased risk of developing ovarian cancer are recommended to perform regular ultrasounds and CT scans (Coalition, 2023; ESMO, 2017).

1.2 Treatment of Epithelial Ovarian Cancer and The Importance of Platinum-based Chemotherapeutics

The treatment strategy for epithelial ovarian cancer commonly begins with a surgical resection , and the staging of the tumor, followed by systemic chemotherapy. Platinum-based chemotherapeutics such as cisplatin and carboplatin play a pivotal role in chemotherapy regimens. Stage of the disease is a key factor that is taken into consideration to design an effective chemotherapy regimen and to decide whether other anti-cancer agents should also be combined with platinum-based chemotherapeutics (ESMO, 2017).

Women who are diagnosed at Stage I of epithelial ovarian cancer express a high risk of recurrence, therefore, following surgery, they are treated with chemotherapy, most commonly, carboplatin. In regards to women who are diagnosed in later stages, a standard combined therapy regimen is commonly used, typically consisting of one treatment session every three weeks for a total of six sessions (ESMO, 2017).

The risk of reoccurrence, metastasis and degree of platinum drug resistance also determines the types of anti-cancer drugs used in the treatment regimen. In regards to rate of recurrence, early relapse of the disease is treated with a single chemotherapeutic while late relapse is approached by a carboplatin-based doublet regimen. Alternatively, targeted therapy through a vascular epidermal growth factor antagonist bevacizumab is used in combination with carboplatin and paclitaxel and gemcitabine or carboplatin. Combined paclitaxel and carboplatin or docetaxel/doxorubicin and carboplatin is the treatment regimen for tumors that have locally metastasized. However, for tumors that have metastasized at a larger scale, bevacizumab is introduced in combination with paclitaxel or carboplatin. Finally, patients that have developed platinum resistance are treated with paclitaxel, topotecan or pegylated liposomal doxorubicin combined with bevacizumab (ESMO, 2017).

1.3 The Mechanism of Action of Cisplatin

Cisplatin is a widely used chemotherapeutic drug used to treat, lung, and bladder cancer. It is also a commonly used platinum-based agent in the treatment of ovarian cancer (Ghosh, 2019).

Within the chemical structure of cisplatin is a central platinum ion, with two ammonia groups, and two chloride ions in cis configuration (**Figure 1**). Each component of the chemical structure plays a role in maximizing the effectiveness of cisplatin. As a drug molecule, the presence of the ammonia groups in a cis configuration increases the drug's reactivity in comparison to its' trans configuration (Ghosh, 2019).

As shown in **Figure 1** below, upon the integration of cisplatin into the cell, the chloride ions undergo a process known as aquation, in which one or two ions are replaced by water molecules to form a positive charge. This process increases cisplatin's reactivity. In regards to the core platinum ion, it enables covalent bonding with the nitrogen atoms of purine bases on the DNA strands to form inter and intra cross links (Dasari & Tchounwou, 2014). These links then develop to form structures known as DNA adducts which interrupt transcription through creating DNA breaks. Following this interruption, the cell is left with the decision to carry out an apoptotic cell death or repair the DNA damage through a tumor suppressor protein known as p53 (Makovec, 2019). Therefore, p53 together with its target p21 is a pivotal protein in the mechanism of action of cisplatin. Hence alterations in the function of both p53 and p21 play key roles in resistance to cisplatin. Before delving into these resistance mechanisms and density dependent cisplatin resistance in particular, let's review the importance of p53 and p21 in the mechanism of action of cisplatin and how these molecules are regulated in response to cisplatin treatment.

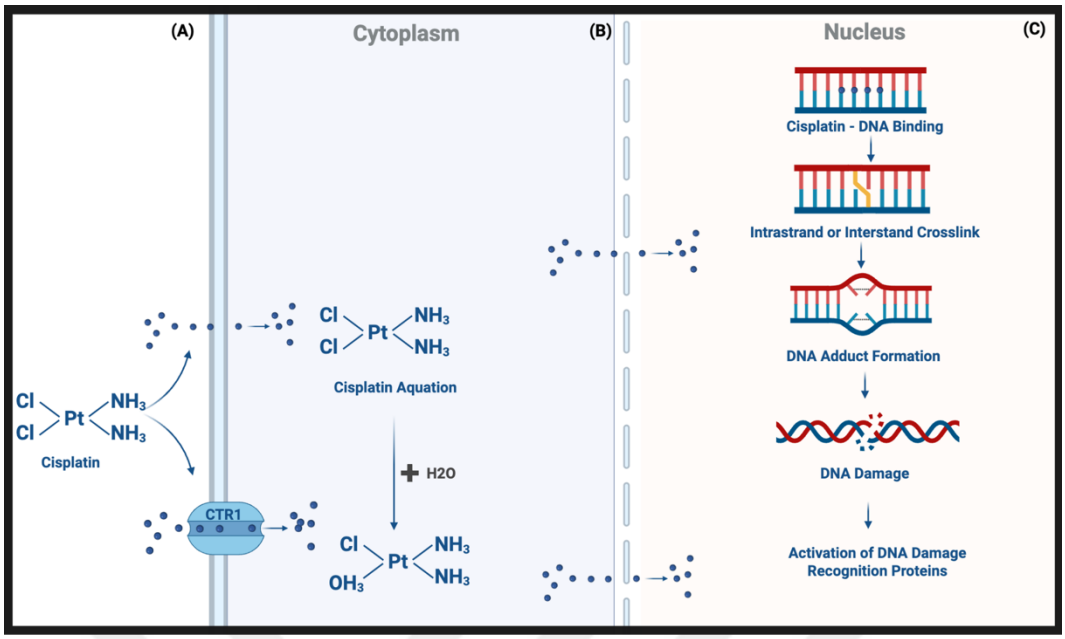

Figure 1: Illustration of the mechanisms by which cisplatin is incorporated into the cell. **(A)** Cisplatin enters the cell through passive transport or active transport by Copper Transporter 1 (CTR1). **(B)** In the cytoplasm, cisplatin molecules undergo aquation. **(C)** Upon reaching the nucleus, cisplatin binds to DNA, forms DNA adducts through intrastrand or interstrand crosslinks, and results in DNA damage. DNA damage recognition proteins are then activated and trigger tumor suppressor p53 either initiates p21 mediated cell cycle arrests and DNA repair or apoptotic cell death.

1.3.1 The Importance of p53 in Cisplatin's Mechanism of Action

Tp53 is a tumor suppressor gene acting as one of the important regulators in the human genome and encoding p53, a protein known to control a multitude of pathways involving genome stability, cellular fate and DNA damage response. As a result of the importance p53 plays in responding to DNA damage, 50% of cancer types have been found to express mutations in Tp53. Additionally, research shows that p53, whether in the mutated or wildtype form, highly contributes to chemoresistance in cancer patients (Marei et al., 2021).

In response to the DNA damaging crosslinks produced by cisplatin, p53 is activated. Due to its role in determining cellular fate, p53 initiates the transcription of downstream targets that promotes cell cycle arrest, DNA repair, or apoptosis, depending on the extent of DNA damage (Siddik, 2003).

1.3.2 The Structure of p53

p53 consists of four main domains, which include two transactivating motifs, a DNA binding domain, and a tetramerization motif (**Figure *2***). The domains in close proximity to the N-terminal, the transactivating domains, are involved in the regulating the transcriptional capacity of p53. Conversely, domains in the vicinity of the C-terminal, both the DNA binding domain and the tetramerization motif, regulate p53's DNA binding ability. Additionally, the tetramerization motif also contributes to other functions such as protein-protein interactions and p53 degradation (Hafner et al., 2019). Studies have shown that the tetramer form of p53 contributes to the nuclear accumulation of the protein by masking it's nuclear export signal (O'Brate & Giannakakou, 2003). The interaction of proteins relevant to the domains is not the only regulators of p53's function. Post translational modifications, most importantly phosphorylation, ubiquitylation, and acylation play an essential role in the differential functions of p53 (Hafner et al., 2019).

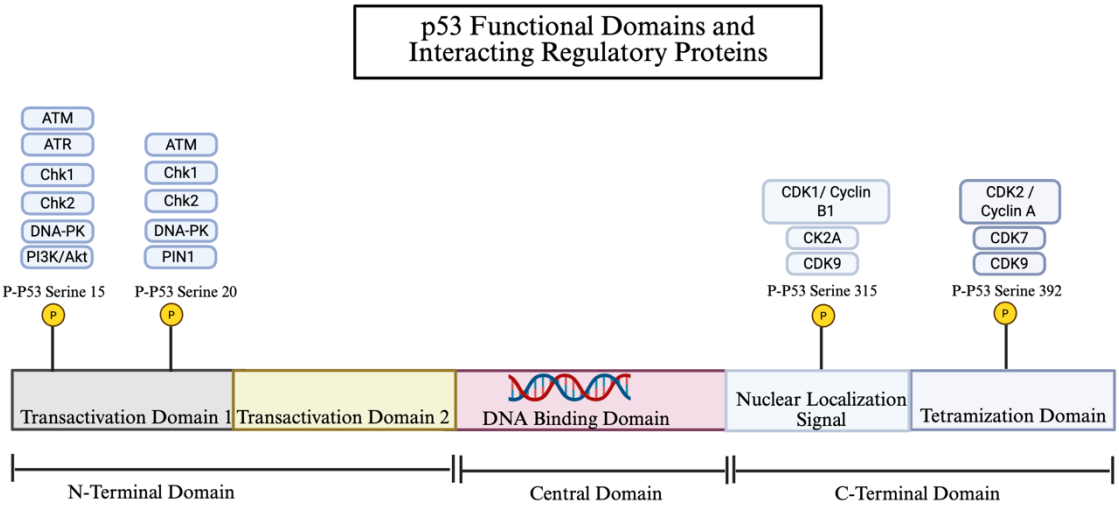

Figure 2: Representations of p53 functional domains and associated regulatory protein interactions. Phosphorylated p53 sites Serine-15 and Serine-20 lie within the C-terminal domain at the first transactivation domain. Serine-315 and Serine-392 sites lie within the C-terminal domain at the nuclear localization signal and tetramerization domain respectively. Each phosphorylation site is regulated by proteins shown in blue above each site.

1.3.3 The Functions of p53: Cell cycle arrest, DNA repair, and Apoptosis

Under normal conditions p53 acts as a transcription factor, maintaining homeostasis. However, as a result of stressful stimuli, p53 can induce cell cycle arrest, DNA repair, or apoptosis in accordance with the proteins it interacts with and the post-translational modifications it undergoes (Hernandez Borrero & El-Deiry, 2021).

Cyclin Dependent kinase inhibitor, p21, Proliferating Cell Nuclear Antigen (PCNA), and Growth Arrest and DNA Damage-inducible 45 alpha (GADD45a) are proteins transcribed by p53 that induce cell cycle arrest at different phases of the cell cycle. While p21 can activate cell cycle arrest at multiple phases, when induced by p53, it primarily induces cell cycle arrest at G1/S. Similarly, GADD45a activates cell cycle arrest at G1/S along with G2/M. In regards to PCNA, when transcribed by p53, it results in the inhibition of DNA replication (Hernandez Borrero & El-Deiry, 2021).

Research has also shown that p53 is involved in the activation of both apoptotic forms, intrinsic and extrinsic apoptosis. In the extrinsic form of apoptosis, p53 induces the transcription of the Fas/FasL receptor which in return activates caspase-8 and caspase-3, and apoptosis (Hernandez Borrero & El-Deiry, 2021) .In regards to intrinsic apoptosis, p53 can either transactivate pro-apoptotic proteins Bax, Bak, Bid, Noxa, Puma or directly interact with them on the mitochondria. Regardless, both can result in the activation of the caspase cascade, and apoptosis (Hernandez Borrero & El-Deiry, 2021).

1.3.4 The Regulation of p53: Interacting Proteins, Phosphorylation Pattern, and Subcellular localization

Interacting upstream proteins are the first essential regulators of p53's function. These proteins are able to directly or indirectly interact with p53. Indirectly modulating p53's function takes place through affecting Mouse double minute 2 homolog (MDM2), p53's negative regulator (Hafner et al., 2019).

The post translational modification (PTM), phosphorylation, is the second factor considered upon identifying the differential functions of p53. Phosphorylation is a crucial PTM that is determined by a number of proteins interacting with p53 at different phases of the cell cycle. Additionally, p53 undergoes different phosphorylation patterns in response to upstream stimuli including stress and DNA damage. Furthermore, the domains that p53 is phosphorylated on the N-terminal and C-terminal contributes to its function. As show in **Figure 2** Phosphorylation sites closer to the N-terminal, such as Serine-15 and Serine-20 regulate the transcriptional activity of p53 and its stability. On the other hand, phosphorylation sites closer to the C-terminus such as Serine-315 and Serine-392 contribute to p53's subcellular localization, tetramer formation, and DNA binding. (Hafner et al., 2019).

Together, the phosphorylation pattern of p53 and the proteins interacting with it give rise to the third factor regulating p53's function, subcellular localization. Under normal conditions, p53 is expressed at very low levels in the nucleus and is continuously degraded in the cytoplasm. However, in the presence of DNA damage, nuclear levels of p53 increase, enhancing its ability to regulate the transcription of downstream proteins. Nonetheless, when the DNA damage is unrepairable, p53 can translocate to the mitochondria where it can induce intrinsic form of apoptosis (O'Brate & Giannakakou, 2003).

1.3.5 *Proteins that Regulate p53 function*

MDM2, ATM, & ATR

Ataxia-Telangiectasia mutated (ATM) and Ataxia Telangiectasia and Rad3-related (ATR) are proteins belonging to the phosphatidylinositol 3-kinase-like family of serine/threonine protein kinases (PIKKs). While their functions are closely related, the main difference between them is the stimuli prompts their activation. ATM specifically responds to double stranded breaks and ATR responds to a broader range of DNA damage, particularly ones that result in single stranded DNA breaks, normally occurring due to stalling of the replication fork (Smith et al., 2020).

As mentioned above, ATM and ATR play an important role in controlling cell cycle progression mainly through initiation of cell cycle arrest at G1, S and & G2/M. The mentioned cell cycle arrest is carried out by downstream targets of ATM and ATR, Checkpoint Kinase 1 (Chk1) and Checkpoint Kinase 2 (Chk2). Additionally, Chk1 and Chk2 also contribute to the phosphorylation of p53 at Serine-15 and Serine-20 (Smith et al., 2020).

Under normal conditions, p53 is actively exported from the nucleus to the cytoplasm for proteasomal degradation by its negative regulator, MDM2 . However, the relationship between MDM2 and p53 requires a balance in the expression of both proteins, as shown in **Figure 3**. Therefore, p53 activates MDM2 as part of negative feedback loop, preventing excessive p53 production (**Figure 3. A,B**). When the cell undergoes DNA damage, initial damage recognition protein, ATM phosphorylates MDM2, hindering its ability to export p53 to the nucleus. Following that, ATM and ATR initially phosphorylate p53 at Serine-15 , leading to its activation through Chk2. The phosphorylation at Ser-15 subsequently triggers the phosphorylation of p53 at Ser-20 also by Chk2. The region where ATM and ATR bind to p53 overlaps with MDM2's binding site on the transactivation motif of p53. Therefore, upon phosphorylation at Ser-15 and Ser20, the bond between MDM2 and p53 is broken, permitting an increase in p53's nuclear levels (Smith et al., 2020). Finally, in accordance with the phosphorylation pattern and extent of DNA damage, p53 can induce cell cycle arrest, DNA repair, or apoptosis (**Figure 3. C)**.

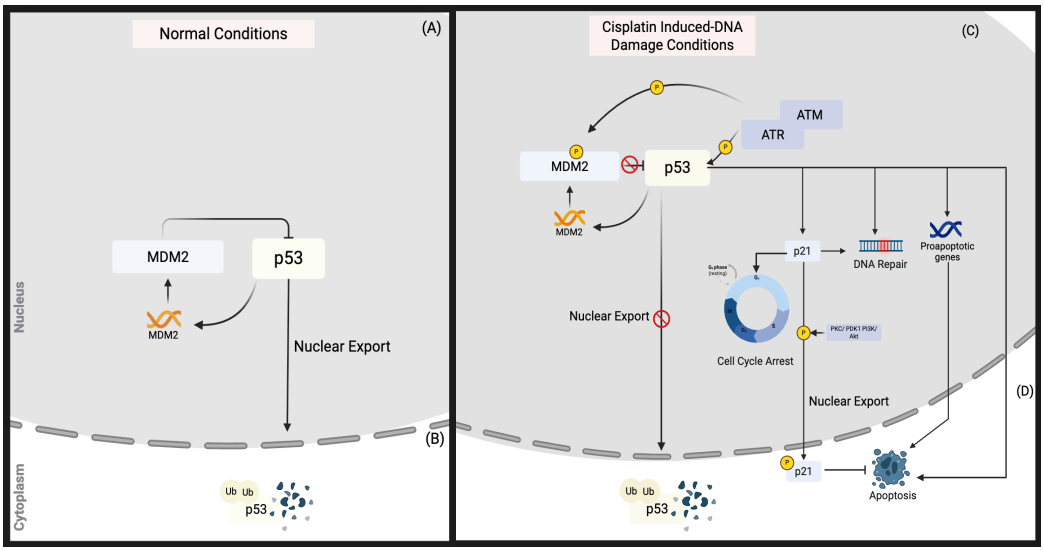

Figure 3: The regulation of p53 by ATM, ATR and MDM2 under normal and stressed conditions. **(A)** Under normal conditions, negative regulator, MDM2 induces the export of p53 to the cytoplasm. **(B)** Ubiquitin mediated degradation of p53 takes place. **(C)** ATM and ATR phosphorylate MDM2 and inhibit ubiquitin mediated degradation of p53 in the cytoplasm. p53 then accumulates in the nucleus and transactivates target genes to induce p21 mediated cell cycle arrest, DNA repair, or apoptosis. **(D)** p21 can also be exported to the cytoplasm to inhibit apoptosis while p53 can induce apoptosis in the cytoplasm.

Peptidyl-prolyl cis/trans isomerase (PIN1)

Peptidyl-prolyl cis/trans isomerase (PIN1) is a proline directed serine/threonine phosphatase that was found to contribute to the ATM mediated stabilization of p53 in the presence of DNA damage. Through interacting with the Serine-315 phosphorylation site of p53, PIN1 increases the affinity of Chk2 to p53. In return, an increase in the phosphorylation of p53 at Ser-20 by Chk2 takes place and stabilizes the protein (Cheng & Tse, 2018).

Cyclin Dependent Kinases: CDK1/CDK2/CDK7/CDK9

A family of serine/threonine kinases known as cyclin dependent kinases (CDKs) are known to be responsible for cell cycle progression. By phosphorylating target proteins, CDKs are able to effectively regulate the cell cycle at each of its phases. One of these targets protein includes p53. CDK1, CDK2, CDK7, and CDK9 are some CDKs that phosphorylate p53 throughout different cell cycle phases and checkpoints (Friedrich Marks, 2017).

In regards to CDK1, studies have shown that when in a complex with Cyclin B1 and under stressful conditions, the CDK is able to phosphorylate p53 at serine-315. This modification hinders p53's ability in activating mitochondrial apoptosis (Nantajit et al., 2010). A second cyclin dependent kinase, CDK2, is also able to phosphorylate p53 on the serine-392 residue in the presence of stress when in a complex with cyclin A. The outcomes of this phosphorylation include, enhancing p53's binding to transcriptional coactivators, stabilizing p53 (Blaydes et al., 2001), and strengthening p53's DNA binding ability (POSPÍŠILOVÁ et al., 2004). Moreover, similarly to phosphorylation by CDK2, CDK7 induced phosphorylation of p53 on serine-392, elevates the protein's DNA binding ability. This specifically takes place when CDK7 is in a complex with cycH (cyclin H) and regulatory protein p36 (Lu et al., 1997). Lastly, A study using mass spectrometry reveled that the Cyclin T1/ CDK9 complex phosphorylates p53 at both serine-315 and serine-392 residues. The researchers claimed that phosphorylation at these sites promote the interaction of p53 with Pin1. This interaction is then followed by conformational change which elevates the protein's DNA binding ability (Radhakrishnan & Gartel, 2006).

Casein Kinase II (CK2)

In addition to CDKs, another set of serine/threonine kinases known as Casein kinases (CKs) are involved in the phosphorylation of p53 the serine-392 residue. In the context of regulating p53 activity, CK2 has contradictory functions relevant to the resultant phosphorylation pattern. p53 accumulation is inhibited by CK2 mediated MDM2 phosphorylation in unstressed conditions. Conversely, CK2

phosphorylates p53 at Ser392 in stressed conditions enhancing the tetramerization of the protein, and promoting the accumulation of serine-392 phosphorylated form (Meek, 2013). Another study also showed that CK2A does indeed phosphorylate p53 at serine-392, however, the researchers claim that this phosphorylation event is not sufficient to protect p53 from Human Double Minute 2 (HDM2) inhibition (Kapoor et al., 2000). Finally, another study provided evidence which supports the inadeqeunce of CK2A mediated phosphorylation of p53 when compared to CDK2/cyclin A mediated phosphorylation (POSPÍŠILOVÁ et al., 2004)

DNA Protein Kinase (DNA-PK) & Chk2

As mentioned above, Chk2 plays an essential role in the phosphorylation of p53 through upstream signals from ATM and ATR. In addition to this role, a study has shown that DNA-Protein Kinase (DNA-PK) and Chk2 act in synergism to phosphorylate p53 at Ser-20. Similarly to phosphorylation by other kinases, DNA-PK and Chk2 promote the stability of p53. However, the mentioned study has also highlighted the importance of DNA-PK in Non-Homologous End Joining (NHEJ). Since Chk2 is involved in cell cycle arrest, the kinases may synergize to simultaneously trigger cell cycle arrest and repair DNA damage through NHEJ (Jack et al., 2004).

PI3k/Akt

Phosphatidylinositol 3-Kinase/ Protein kinase B (PI3K/Akt) pathway regulates p53 through two main mechanisms. Firstly, PI3k phosphorylates and upregulates MDM2, hence increasing the nuclear export and degradation of p53. Secondly, in response to DNA damage, Akt1 phosphorylates p53-related protein kinase (PRPK) which in return phosphorylates p53 at Serine-15 (Facchin et al., 2007). Moreover, another study reported that the phosphorylation of ovarian cancer cell line, A2780, by PI3k/Akt in response to cisplatin treatment is essential for the activation of p21 in a p53 dependent manner. However, the site of phosphorylation is not clear. (Mitsuuchi et al., 2000)

Table 1: Regulation of p53 Phosphorylation in Response to Cellular Stress

Phosphorylation site	Domain / Terminus	Kinase / Regulatory Protein	Functional Outcome
Serine 15	Transactivation domain / N-terminus	ATM ATR Akt1	Increases nuclear p53 accumulation and stability *(Smith et al., 2020)* Increases nuclear p53 accumulation and stability *(Smith et al., 2020)* Increases nuclear p53 accumulation and stability *(Facchin et al., 2007)*
Serine 20	Transactivation domain / N-terminus	ATM ATR PIN1 DNA-PK	Increases nuclear p53 accumulation and stability *(Smith et al., 2020)* Increases nuclear p53 accumulation and stability *(Smith et al., 2020)* Stabilizes p53 *(Cheng & Tse, 2018)* Cell cycle arrest a& Non Homologous End Joining mediated repair *(Jack et al., 2004)*
Serine 315	Nuclear Localization Signal / C-terminus	PIN1 Cyclin B1/Cdk1 Cyclin T1/ Cdk9	Stabilizes p53 *(Cheng & Tse, 2018)* Inhibits mitochondrial Apoptosis *(Nantajit et al., 2010)* Stabilizes p53 *Radhakrishnan & Gartel, 2006)*
Serine 392	p53 Tetramerisation motif/ C-terminus	Cyclin A/Cdk2 Cyclin H/ Cdk7 Cyclin T1/ Cdk9 CK2	Enhances binding to transcriptional coactivators *(Blaydes et al., 2001)* Stabilizing p53 *(Lu et al., 1997)* Stabilizes p53 *(Radhakrishnan & Gartel, 2006).* Accumulation of p53 in the phosphorylated and tetramer form *(Meek, 2013)*

1.3.6 The Importance of p21 in Cisplatin's Mechanism of Action

As a part of the cip/ kip family of cyclin dependent kinase inhibitors, p21 is responsible for inhibiting the cell cycle at specific checkpoints including G1/S and G2/M. Activation of p21 can take place both directly or indirectly through upstream pathways in response to various stimuli including, oxidative stress, DNA damage, cytokines and mitogens, tumors and viruses, and anticancer agents such as cisplatin (Karimian et al., 2016). In response to the DNA damaging crosslinks produced by cisplatin, p21 is either activated by p53 or through other pathways involving SMADs, STATs or BRCA1. Depending on the extent of damage and cellular context, p21 can be upregulated to induce cell cycle arrest and facilitate DNA repair; however, if the damage is irreparable, p21 is downregulated and p53 may promote apoptosis (Siddik, 2003).

1.3.7 Functions of p21: Cell cycle arrest, DNA repair, and Apoptosis

Induction of cell cycle arrest by p21 occurs through two main mechanisms. Firstly, p21 can inhibit the phosphorylation activation of CDKs and cyclin complexes, CDK4,6/Cyclin-D and CDK2/Cyclin-E at G1/S and G2/M respectively. Secondly, p21 can compete with DNA polymerase **δ** for binding to Proliferating Cell Nuclear Antigen (PCNA), resulting in the inhibition of transcription. The binding of p21 to PCNA does not always inhibit the activity of PCNA as it is responsible for mediating DNA damage repair mechanisms such as Base Excision Repair (BER), Nuclear Excision Repair (NER), Mismatch Repair (MMR), and Translesion DNA Synthesis (TLS) (Jung et al., 2010). When required, p21 can arrest the cell cycle while enabling PCNA-mediated DNA damage repair. In other cases, p21 can also arrest the cell cycle and inhibit these forms of repair by preventing PCNA from binding to the relevant repair components (Y. S. Jung et al., 2010) While p21 is known to function in cell cycle arrest, studies show that p21 also acts as an inhibitor of apoptosis in the cytoplasm, where it binds to and inhibits apoptotic executioner caspase-3 (Cmielova & Rezacova, 2011).

1.3.8 The Regulation of p21: Interacting Proteins, Phosphorylation Pattern, and Subcellular localization

The relationship between p21 and p53

Treatment with chemotherapeutics and expression of oncogenic Ras are upstream stimuli that result in p53 induced p21 mediated cell cycle arrest. When the cell is under repairable DNA damage, p53 is localized in the nucleus where it transcribes CDKN1A, the gene encoding for p21. P53-mediated upregulation of p21 enables cell cycle arrest at G1/S and G2/M to maintain genomic stability and the prevention of proliferation of damaged cells (Karimian et al., 2016).

Cytoplasmic translocation of p21 by PI3K/Akt, PKA, and PKCζ

Under extensive DNA damage conditions, procaspase-3 cleaves and inhibits cytoplasmic p21 to activate Transforming Growth Factor β (TGF-β) mediated apoptosis (Y. S. Jung et al., 2010). However, cytoplasmic p21 has also been shown to express antiapoptotic and oncogenic functions. Anti-apoptotic functions typically arise in repairable DNA damage conditions. Contrarily, oncogenic functions may be a result of mutations or chemoresistance in cancer cells. The upregulation of cytoplasmic p21 levels is controlled by upstream phosphorylation through a number of proteins (Karimian et al., 2016).

Phosphatidylinositol 3-Kinase (PI3K/Akt) is one of the pathways responsible for the cytoplasmic localization and stability of p21 through phosphorylation at Threonine-145 and Serine-146 sites. Evidence has shown that phosphorylation of p21 by Akt at Threonine-145, has a number of downstream implications. Firstly, the phosphorylation event prevents the inhibitory binding of CDK2 and PCNA, enabling the progression of the cell cycle. Secondly, the cytoplasmic levels of p21 increase and enable the inhibition of apoptosis by binding to pro-apoptotic proteins such as caspase-3 and caspase-8. Similarly, phosphorylation of p21 at Threonine-145 by Protein Kinase A (PKA) inhibits Fas/FasL induced extrinsic apoptosis by inhibition of procaspase-3 (Y. S. Jung et al., 2010).

Furthermore, studies have demonstrated that PI3K/Akt phosphorylates p21 at Serine-146 indirectly through Protein Kinase C ζ (PKCζ). This results in cell cycle progression past the G1/S cell cycle arrest in the presence of mitogenic stimuli (Y. S. Jung et al., 2010). Despite abundant evidence regarding the antiapoptotic role of p21 when phosphorylated on Threonine-145 and Serine-146, other studies have shown contradictory results. For instance, phosphorylation of p21 at Serine-146 by PDK1 activated PKCζ induces p21 degradation in the cytoplasm (Al Bitar & Gali-Muhtasib, 2019). Therefore, the function of p21 relevant to its phosphorylation pattern was demonstrated to be context dependent (Abbas & Dutta, 2009).

Nucleic localization of p21

Growth inhibitory function of p21 has been associated with its nuclear localization. In the nucleus, p21 expresses its antiproliferative effects through cell cycle arrest. As mentioned above, p21 can interact with PCNA in the nucleus to block DNA replication. In addition to PCNA, p21's interaction Growth Arrest and GADD45A also enhances cell cycle arrest. While PCNA and GADD45A interact with p21 to enhance its function, upon interaction with MDM2 in the nucleus, p21's stability is reduced (Cmielova & Rezacova, 2011).

Table 2: Regulation of p21 Phosphorylation in Response to Cellular Stress

Phosphorylation site	Kinase	Functional Outcome
Threonine -145	PI3K/Akt	Stabilizes p21 and contributes to its cytoplasmic localization *(Y. S. Jung et al., 2010)* Enables progression of the cell cycle *(Y. S. Jung et al., 2010)*
	PKA	inhibition of apoptosis by binding procaspase 3 and procaspase 8 *(Y. S. Jung et al., 2010)* inhibits Fas/FasL extrinsic apoptosis by inhibition of caspase-3 *(Y. S. Jung et al., 2010)*
Serine -146	PDK1/PKCζ	Degradation of p21 *(Al Bitar & Gali-Muhtasib, 2019).*
	PI3K/Akt/ PKCζ	Enables Cell cycle progression past the G1/S cell cycle arrest *(Y. S. Jung et al., 2010).*

1.4 *Cisplatin Resistance and Underlying Mechanisms*

Cisplatin is one of the most commonly used chemotherapeutic to treat ovarian cancer. As a platinum-based drug, cisplatin is able to covalently bind to DNA, forming adducts, inhibiting transcription, and resulting in cell death. However, cancer cells may develop resistance towards cisplatin via intracellular changes. For instance, resistance to chemotherapy takes place when cells are no longer able to initiate

apoptosis in response to DNA damage. This apoptotic escape decreases the cells' sensitivity towards chemotherapeutic drugs, posing as a major obstacle towards cisplatin-based treatment of ovarian cancer Besides this, resistance to cisplatin may develop through several other mechanisms including decreased drug influx, increased drug efflux, intracellular inactivation of the drug and increased DNA damage repair (Chen & Chang, 2019).

1.4.1 Decreased Drug Influx via Copper Transporter 1&2 (CTR1 & CTR2)

The uptake of cisplatin takes place through two main mechanisms, passive and active diffusion. Copper Transporter 1 (CTR1) is the primary membrane protein involved in active transport of cisplatin into the cell. The key physiological function of CTR1 is the uptake of copper ions to maintain cellular homeostasis. However, studies have shown that CTR1 can be involved in the uptake of platinum-based drugs such as cisplatin (Chen & Chang, 2019). Moreover, recent evidence suggests that aside from its plasma membrane form, CTR1 is endocytosed into vesicles, suggesting another possible mechanism in which cisplatin is incorporated into the cell (Schoeberl et al., 2022) (Siddik, 2003). In addition to CTR1, research has shown that Copper Transporter 2 (CTR2) also plays a role in cisplatin uptake in which it functions in an interdependent manner with CTR1 manner to regulate cisplatin uptake (Anna Schoeberl et al., 2022). Another study by portrayed the independent function of CTR2, in which upon knocking out the gene, cisplatin uptake drastically increased, shedding light on the possible involvement of CTR2 in cisplatin resistance (Ali et al., 2022). Finally, an additional study reported that the ratio of CTR2 to CTR1 acts as a prognostic factor for cancer patients in which higher ratios are associated with resistance to platinum containing chemotherapeutics (Öhrvik & Thiele, 2015).

1.4.2 Increase in Cisplatin Efflux

ATPase copper-transporting alpha (ATP7A) and ATPase copper-transporting beta (ATP7B) are two efflux transporters that maintain copper ion balance in the cell. Similarly to CTR1, ATP7A and ATP7B both express the ability to transport cisplatin along with copper ions. Studies have shown that overexpression of these ATPase genes was correlated with poor cisplatin treatment response in ovarian cancer, indicating a possible role of ATP7A and ATP7B in cisplatin resistance through enhanced drug efflux (Chen & Chang, 2019) (Siddik, 2003). Aside from cisplatin efflux, studies have shown that the proteins are also able to act in other mechanisms to mediate resistance. For instance, ATPP7A and ATP7B are able to sequester the drug inside the cell in an unreactive form. Overall, high expression of efflux transporters, ATP7A and ATP7A is associated with resistance to various chemotherapeutic agents including cisplatin (Lukanović et al., 2020).

1.4.3 Intracellular Inactivation of Cisplatin

In order for cisplatin to enter the cell, it has to go through the process of aquation which replaces one or two of its chloride ions with water. Following that, cisplatin interacts with two thiol-containing molecules that facilitate its activation, Glutathione (GSH) and metallothionein. While these molecules are required for cisplatin activation, their upregulation has been linked to cisplatin resistance, as they prevent the drug from binding to the target DNA (Chen & Chang, 2019) (Siddik, 2003).

1.4.4 Increased DNA damage repair

As mentioned above, the hallmark of chemoresistance is the inability of cancer cells to go into apoptosis after treatment. Increased DNA damage repair is one of mechanisms in which cells can escape apoptosis by favoring post-replication rather than pre-replication repair (Chen & Chang, 2019).

Nucleotide Excision Repair (NER)

NER is the main biological process used to repair DNA adducts which are formed by cisplatin. By excising the damaged section of DNA and refilling the gap with the

correct nucleotides, the region is restored to its correct form. While many proteins are involved in this process, Excision Repair Cross-Complementation Group 1(ERCC1), ERCC1/ Xeroderma Pigmentosum Complementation Group F (XPF) complexes, and Xeroderma Pigmentosum Complementation Group A (XPA) are notably expressed in cisplatin resistant tumors. In particular, overexpression of ERCC1 was correlated with poor response to cisplatin in ovarian cancer patients (Chen & Chang, 2019) (Siddik, 2003).

Homologous Recombination

Once NER is unable to repair DNA adducts efficiently, double stranded DNA breaks occur and result in the activation of a second form of adduct repair, homologous recombination. Breast Cancer Type 1 and 2 (BRCA1 & BRCA2) are the two fundamental genes responsible for homologous repair. Therefore, ovarian cancer tumors with a BRCA1 or BRCA2 are unable to repair double stranded breaks and were shown to respond effectively to cisplatin treatment (Chen & Chang, 2019)

1.4.5 Dysregulation of the Apoptotic Pathway

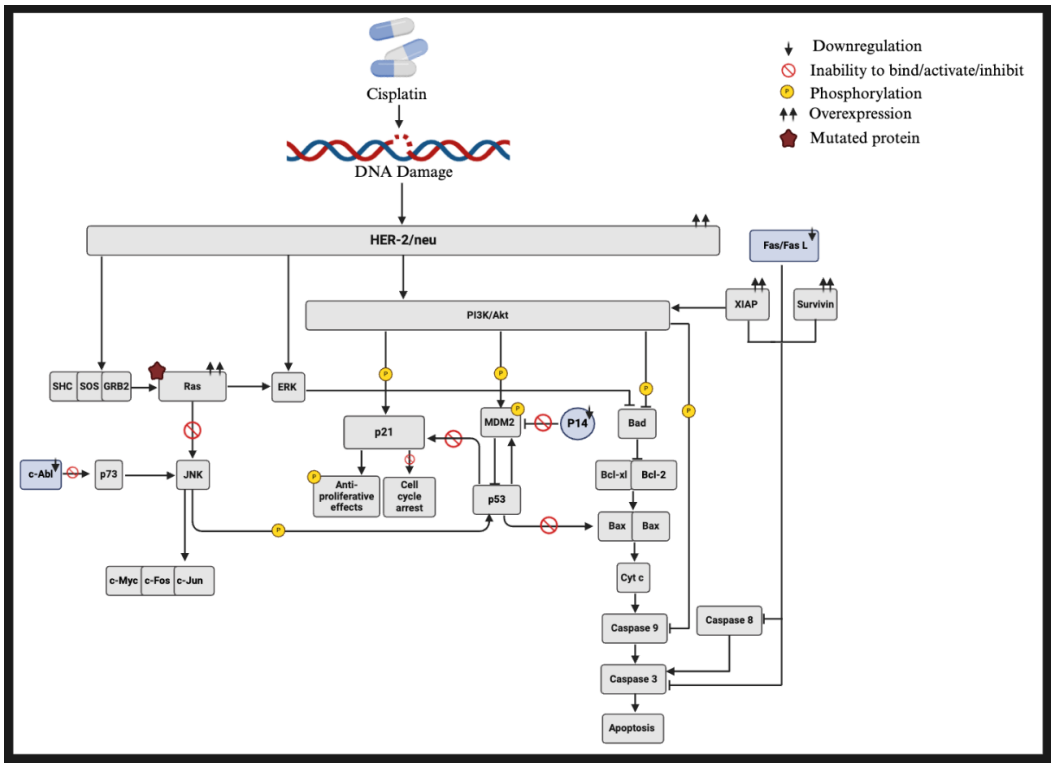

Figure 4: The crosstalk between cisplatin induced DNA damage pathways and the mechanism resulting in resistance. Her-2/neu overexpression is one of the hallmarks of cisplatin resistance which targets downstream effectors independently and through PI3K/Akt. These events mediate resistance through increasing p53 levels, inhibiting the intrinsic and extrinsic apoptotic pathways, and inhibiting p21 mediated cell cycle arrest. This figure was adapted from (Siddik, 2003).

Receptor tyrosine-protein kinase erbB-2 (Her2-neu) is a protein that is involved in cellular growth and proliferation. As shown in

Figure *4* above, the overexpression of HER-2/neu has been found to support the development of cisplatin resistance due to disrupted downstream pathways. PI3K/Akt is one of the main targets of HER-2/neu. In response to cisplatin, the PI3K/Akt phosphorylates p53 resulting in subsequent activation of p21 mediated cell cycle arrest. However, the overexpression of Her-2/neu or X Inhibitor of Apoptosis Protein (XIAP) results in the upregulation of PI3K/Akt and development of cisplatin resistance as follows (Siddik, 2003).

Firstly, PI3K/Akt, can indirectly diminish the levels of p53 by phosphorylating MDM2, enabling it to bind strongly to p53. Amplifying this effect can also take place through the inability of p53 regulator, p14, to inhibit MDM2 activity. Diminishing the levels of p53 prevents appropriate apoptotic or DNA damage responses such as activation of Bax and p21 respectively. However, similar outcomes can arise from p53 mutations. Secondly, PI3/Akt can interact with p21 by phosphorylating it at Thr145 resulting in antiproliferative cellular effects. Thirdly, PI3K/Akt can act on the intrinsic apoptotic pathway by phosphorylating Bad or Caspase-9, leading to the inhibition of pro-apoptotic activity (Siddik, 2003).

In addition to PI3K/Akt, overexpression of Her-2/neu activates the Ras/MAPK kinase pathway through activation of SHC/SOS/GRB. Upon the upregulation or mutation of Ras, a number of alterations take place. Primarily, when ERK is activated by Ras, it can lead to the inhibition of Bad, preventing the initiation of pro-apoptotic activity. Moreover, JNK is a second target of ERK and a main target for c-Abl/p73. The improper activation of JNK by c-abl/p73 downregulation or dysfunctional Ras

prevents the phosphorylation of p53 and activation of c-Myc,c-Fos, and c-Jun transcription factors (Siddik, 2003).

Independently of Her-2/neu pathway, downregulation of the extracellular apoptotic pathway regulator, Fas/FasL results in the inactivation of Caspase-3 and caspase-8. Additionally, overexpression of pro-apoptotic proteins survivin and XIAP result in a response parallel to downregulation of Fas/FasL. In summary, dysregulation of the damage response pathways in response to overexpressed Her-2/neu is one of the major cisplatin resistance determinants, with p53 and p21 being two essential impaired targets (Siddik, 2003).

1.5 Cell Density Dependent Cisplatin Resistance

Cisplatin has been long recognized as the main therapeutic agent used to treat ovarian cancer; however, as time progressed, it became evident that the use of cisplatin to treat ovarian cancer is accompanied with major obstacles such as, lack of early detection markers and a high rate of chemo resistant recurrent tumors. Therefore, researchers have been extensively investigating the mechanisms of chemoresistance, particularly in relation to cisplatin (Chen & Chang, 2019).

One of the novel modes of cisplatin resistance defined is cell density or cell confluence dependent cisplatin resistance. Yifeng He and colleagues observed an increase in cisplatin IC50 values (inhibitory concentration needed to inhibit 50% of cell population) with increasing cellular densities (He et al. 2016).

Using five ovarian cancer cell lines including, A2780 and A2780DR, the researchers implemented a limiting dilution assay and an immunohistochemistry-based scoring system for pAkt and p62. Higher cells densities led to reduced levels of autophagy marker p62 and increased levels of survival pathway marker pAkt indicating resistance to cisplatin-induced cell death. Overall, this study was able to correlate cellular density levels with chemoresistance through IC50 measurements, cellular proliferation markers, and cell death indicators (He et al., 2016).

Ujwal Punyamurtula and colleagues have also examined the differential IC50 measurements in ovarian cancer cell lines, TOV-21G and OVMANA. Using a term known as IC50-Seeding Density Slope (ISDS), they were able to consider the density dependent factors that influence differential responses to cisplatin (Punyamurtula et al., 2023). The results showed that the IC50s of the cell lines increased at higher cellular densities when exposed to cisplatin, indicating greater resistance towards the drug. Furthermore, a cell death assay using ethidium homodimers revealed a lower fluorescence intensity in high cell density populations, as opposed to low density populations, demonstrating decreased cell death in response to cisplatin. Deeper investigation also revealed that, as cellular density increases, autophagy markers, such as p62, and pro-apoptotic proteins such as Bax and Noxa decrease, while anti-apoptotic proteins, such as Bcl-2 and c-Flip increase. These protein levels demonstrate the cells ability to resist chemotherapy mediated damage. Finally, when combining cisplatin treatment with chloroquine, an autophagy inhibitor, the levels of synergism between the compounds was found to be lower in cells seeded at a high density, indicating increased tolerance towards autophagy. In summary, this study concludes that the IC50 and rate of chemoresistance in ovarian cancer cell lines TOV-21G and OVMANA is strongly influenced by cellular seeding density (Punyamurtula et al., 2023).

Chemoresistance remains a major obstacle to treatment of ovarian cancer in the clinic. The treatment regimen of ovarian cancer patients begins with cytoreductive therapy which attempts to remove as much of the mass as possible, however, this procedure does not always guarantee the elimination of cancer cells. Therefore, adjuvant chemotherapy follows (Punyamurtula et al., 2023).

Despite these findings, the mechanisms of density-dependent cisplatin resistance are not clear. Although p53 and p21 are the key mediators of cisplatin response, whether dysregulation of these proteins is involved in density-dependent cisplatin resistance was not investigated before. Thus, in this thesis, we concentrated on the role of p53 and p21 regulation in a newly defined mode of cisplatin resistance in

ovarian cancer cells. We also addressed whether decreased drug influx may also contribute to density-dependent cisplatin resistance, since cell density may affect the expression of drug influx pumps in ovarian cancer cells (A. Schoeberl et al., 2022).

1.6 Summary and Aim

Treatment of ovarian cancer remains one of the most challenging in oncology due to the development of resistance to platinum-based chemotherapy such as cisplatin. Emerging evidence suggests that elevated confluency levels may contribute to cisplatin resistance in ovarian cancer cells. However, the molecular mechanisms underlying this phenomenon is not known. Therefore, this project aimed to investigate whether DNA damage response elements, p53 and p21, regulate the cell-density dependent response to cisplatin.

Chapter 2:
METHODS

2.1 *Methods*

2.1.1 *Cell Lines*

A2780 (cisplatin sensitive cell line) and CP16 (cisplatin resistant cell line) were cultured in RPMI 1640, with L-Glutamine (Capricorn) supplemented with 10% Fetal bovine serum (FBS) (Biowest) and 1% penicillin/streptomycin (Biowest). The cells were incubated in an environment at a temperature of 37°C and 5% CO_2.
Upon reaching a confluency level of 70-80% at T75 tissue flasks, the cells were passaged with 4mL of trypsin - 0.25% EDTA (Biowest). To assess cell viability and seed at ideal cell seeding density, hemocytometer trypan blue cell exclusion assay was used.

The confluency-based experiments required three different confluency groups, low confluent, full confluence, and over confluent. Therefore, the cell lines were seeded in 10 cm dishes at different densities ranging from 1 million to 5 million cells for 24 hour and 48-hour growth experiments. The cells were then treated with cisplatin and imaged at the day of isolation to assess their confluency levels. For A2780 cell seeding densities of 500,000, 2 million, and 4 million cells per 10 cm dish were used to achieve low confluence, full confluence, and over confluence. For CP16, cell seeding densities of 1 million, 2 million, and 5 million cells per 10 cm dish were used to achieve the same confluence levels.

2.1.2 *MTT Assay*

A2780 cells were seeded in a 96-well plate at the following cell numbers, 100, 200, 300, and 400 cells per well to achieve 25%, 50%, 75%, and 100% confluency levels. Similar confluency levels were achieved in CP16 by seeding the following numbers, 250, 500, 750, and 1000 cells per well. After 24 hours, cells were exposed

to a range of nine different drug concentrations starting from 10μM to 0.02μM for A2780 and 200μM to 0.8 μM for CP16 prepared through 2-fold serial dilutions. Following five days of treatment, MTT was added, and absorbance measurements were performed using spectrophotometry.

2.1.3 Western Blot

1- Protein Extraction

Whole Cell lysate preparation

A2780 and CP16 cells were seeded at optimized cell numbers in 10 cm dishes. After 48 hours of growth, A2780 and CP16 cells were treated with 1uM and 10uM of cisplatin for 24 hours respectively. Subsequently, cells were placed on ice, washed with 3mL of PBS, scraped using 1mL of PBS, and collected into 1.5mL microcentrifuge tubes. The samples were centrifuged at 21,100 g for 10 minutes at 4 degrees. The supernatant was removed, and the resultant pellets were then lysed with RIPA lysis buffer containing 10% protease and 1% phosphatase inhibitors. Following that, the lysed samples were vortexed three times every 5 minutes on ice and the samples were sonicated at an amplitude of 30% for 10 seconds three times at 4 ºC.

Total protein concentration was determined using Bicinchoninic Acid (BCA) protein kit (Thermofisher scientific) following the manufacturer's instructions. Absorbance was measured at 562 nm using a spectrophotometer. A standard curve was generated using the serial dilutions of bovine serum albumin (BSA) standard. Protein lysates (40 μg per sample) were prepared by mixing 4x Laemmli sample buffers containing β-mercaptoethanol and nuclease free water.

Subcellular Fractionation (REAP Method)

A2780 and CP16 cells were seeded at optimized cell numbers in 10 cm dishes. After 48 hours of growth, A2780 and CP16 cells were treated with 1uM and 10uM of cisplatin for 24 hours respectively. Subsequently, cells were placed on ice, washed with 3mL of PBS, scraped using 1mL of PBS and collected into microcentrifuge tubes. The cell suspension was then centrifuged at a temperature of 4°C and a speed of 21.1g for 10 seconds. The resultant supernatant was discarded, and the pellets were lysed with 900µL of NP40 cocktail containing 10% protease inhibitor, 1% NP40, and 1% phosphatase inhibitor. 300µL of the resuspended fraction was transferred to microcentrifuge tubes as "whole cell lysate". The remaining suspension was centrifuged for the second time at a temperature of 4°C and a speed of 21.1g for 10 seconds. Following centrifugation, 300µL of the supernatant was collected to a new microcentrifuge tube as "cytoplasmic fraction". The remaining supernatant was discarded, and the pellet was resuspended with 1mL of the NP40 cocktail. This suspension was then centrifuged for the third and last time at a temperature of 4°C and a speed of 21.1g for 10 seconds. The supernatant was removed, and the pellet which is composed of the nuclear fraction was resuspended with 180µL of β-mercaptoethanol containing Laemmli buffer diluted with NP40. Following that, 100µL of 4X Laemmli was added to the microcentrifuge tubes containing the whole cell lysate and cytoplasmic fraction samples.

2- SDS Page and Transfer:

Protein samples were heated up to 95°C for 5 minutes and loaded onto Mini PROTEAN TGX Precast gels (Bio Rad). Electrophoresis was initially performed 60V until dye front entered separating gel, followed by 120V until complete separation.

Proteins were transferred onto methanol-activated polyvinylidene difluoride (PVDF) membranes using a semi-dry transfer system (Trans -Blot Turbo, Bio rad) for 30 minutes. To ensure the validity of the transfer, the membranes were stained with

Ponceau S. Following that, the membranes are rinsed with TBS-T and blocked with 5% skim milk for 1 hour at room temperature.

3- Primary & Secondary Antibody Incubation:

Blocked membranes were incubated with primary antibodies overnight at 4°C. The following day, membranes were washed with TBS-T for 10 minutes three times and subsequently incubated with the appropriate HRP-conjugated secondary antibody for 1 hour at room temperature. After secondary antibody incubation, the membranes were washed again three times, 10 minutes each using TBS-T.

4- Detection:

Protein detection was carried out using chemiluminescent substrate Forte (Millipore). The membranes were imaged using the LI-COR Odyssey Fc imaging system. Band intensities were quantified using Image J software.

2.1.4 *Quantitative Polymerase Chain Reaction (qPCR)*

Cell Homogenization and RNA Isolation

A2780 and CP16 cells were seeded at optimized cell numbers in 10 cm dishes. After 48 hours of growth, A2780 and CP16 cells were treated with 1uM and 10uM of cisplatin respectively for 24 hours. Subsequently, cells were placed on ice, washed with 3mL of PBS, scraped using 1mL of PBS, and collected into 1.5mL microcentrifuge tubes. The samples were centrifuged at 21,100 g for 10 minutes at 4 degrees. Total RNA was then extracted using the Nucleospin RNA kit (Macherey - Nagel) following manufacturer’s protocol.

cDNA synthesis

The cDNA mixture was prepared by combining 2.5uL of 2mM dNTPs, 1uL of random hexamer, 1000ng of RNA, and nuclease free water to a final volume of 16.5uL. The samples were placed in a T100 Biorad thermocycler and incubated at the following conditions: lid temperature 105°C, 65°C for 5 minutes followed by a hold at 4°C.

Following that, the RT mix was prepared, consisting of 5uL of First strand buffer, 2uL of 0.1M DTT, and 0.5uL of RNase inhibitor. The RT mix was then added to each sample and incubated at room temperature for 10 minutes.

Following this step, 1uL of MuLV RT enzyme was added to each sample and the tubes were loaded again to the T100 Biorad thermocycler for the reverse transcriptase reaction at the following conditions: lid temperature 105°C, incubation at 37°C for 60 minutes, 70°C, for 19 minutes followed by a hold at 4°C. Upon completion, the synthesized cDNA samples were diluted with 75uL nuclease free water and stored at -20°C.

Quantitative PCR Amplification

PCR primer mixture was prepared by combining 90uL of nuclease free water and 5uL of 100nM each of forward and reverse primers. For each set of primer, a master mix was prepared using 10uL of SYBR, 7ul of nuclease free water, and 1uL of the primer mixture. In 96-well PCR plate, 18uL of the prepared master mix and 2uL of cDNA template were added per well. The plate was sealed with optical adhesive films and centrifuged at 1300 rpm for 2 minutes and loaded into qPCR instrument.

2.1.5 Annexin Staining using Muse Cell Analyzer

Cells were seeded in 6-well plates at the following cell numbers 50,000 cells, 250,000 cells, and 500,000 cells per well to achieve desired low confluence, full confluence, and over confluence levels. Following two days of growth, A2780 and CP16 cells were exposed to 1uM and 10uM cisplatin respectively for 3 days. Cell collection and annexin staining was then performed according to the protocol provided by the manufacturer (Muse Annexin V & Dead Cell Kit, Cytek).

2.1.6 Colony Formation Assay

A2780 and CP16 cells were seeded at optimized cell numbers in 96 well plates and grown for 48 hours. Following that, treatment took place using 7 serially diluted cisplatin concentrations beginning from 2.5uM for A2780 and 20uM for CP16. After 24 hours of treatment, the cells were detached, counted, and reseeded into 6 well plates at a density of 500 cells/mL. Once cells at the control group formed colonies on the 12th day of incubation, crystal violet staining was performed following fixation using 4% paraformaldehyde.

Chapter 3:
RESULTS

3.1 *The Effect of Cellular Density on Cisplatin Sensitivity and Apoptosis Levels*

Several studies have reported that the Half-Maximal Inhibitory Concentration (IC50) is sensitive to cell seeding density upon measurement using MTT (He et al., 2016; Punyamurtula et al., 2023). Therefore, in our investigation we wanted to verify if a similar phenomenon is occurring in cisplatin sensitive A2780 ovarian cancer cell line, and cisplatin resistant CP16 cell model, which is the cisplatin resistant cell line developed from A2870. The cells were seeded at 25%,50%,75%, and 100% confluency states and allowed to grow for 24 hours. Following that, the cells were exposed to 9 different drug concentrations for 5 days. The cell survival was assessed with an MTT assay to establish concentration response curves for cisplatin. High seeding cell numbers may cause a bias in survival assays like MTT, due to the saturation of the measurable absorbance from the indicator dye since the detectors have a detection limit. To address this, just before measuring MTT absorbance from the wells, the content of each well was serially diluted with DMSO, and absorbance values were multiplied by the dilution ratio to appropriately measure absorbance at a linear range exempt from saturation effects. Analysis of IC50 values at day 5 using this adjusted MTT method revealed a confluence dependent increase in IC50 values in both cells lines **(Figure 5.A,B)**. However, cisplatin resistant cell line CP16, exhibited a much more prominent confluence dependent increase in IC50 when compared to the cisplatin sensitive cell line A2780 **(Figure 5.C)**

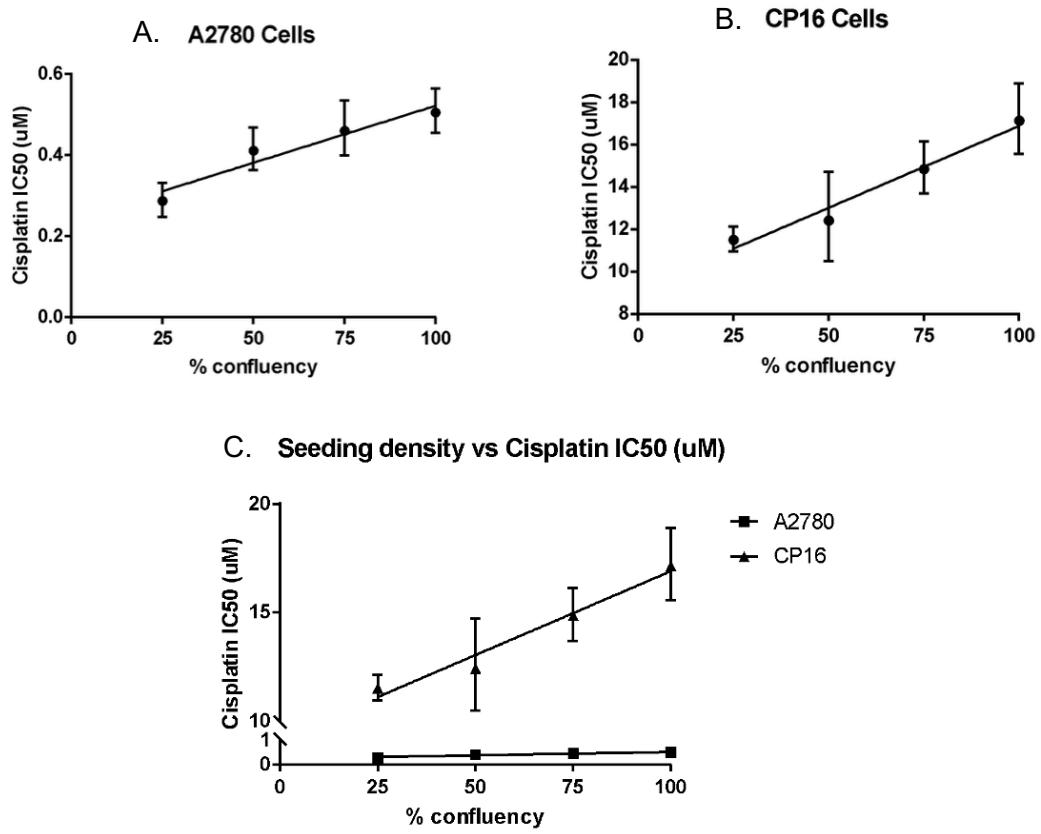

Figure 5: Cisplatin IC50 values of A2780 and CP16 at different confluency levels. (**A)** A2780 and (**B)** CP16 cells were seeded at four different confluency levels (25%,50%,75% and 100%) and allowed to grow for 24 hours. Cells were then exposed to 9 different cisplatin concentrations and IC50 levels were then determined by MTT. **(C)** Comparison of the confluence dependent IC50 levels of A2780 and CP16 in response to cisplatin.

3.2 *Differential Expression of p53 in Accordance with Cellular Confluency*

3.2.1 Subcellular Protein Expression Analysis by Western Blot

After confirming that A2780 and CP16 expressed a confluence dependent increase in cisplatin IC50 values, we continued to investigate whether P53 follows a similar pattern. P53 is one of the main proteins activated upon exposure to cisplatin. In response to the DNA damage that cisplatin induces, nuclear p53 levels increase and promote its function as a transcription factor to induce downstream targets which promote cell cycle arrest, DNA repair, cellular senescence, or transcription dependent apoptosis (Hernandez Borrero & El-Deiry, 2021).Cytoplasmic p53 on the other hand,

is associated with promoting mitochondrial apoptosis, inhibition of autophagy, or MDM2-mediated degradation (Green & Kroemer, 2009).

Because p53 functions are dependent on its subcellular localization, western blotting was performed to detect whole lysate, cytoplasmic, and nuclear p53 levels. Cells were seeded at three different confluency states, low confluent, full confluent and over confluent levels and allowed to grow for 48 hours. Following that, A2780 and CP16 cells were exposed to 1uM and 10uM of cisplatin respectively for 24 hours.

While A2780 expressed a confluence dependent decrease in p53 in whole cell lysates and a slight and statistically insignificant decrease in cytoplasmic p53 levels **(Figure 6.A,C,E)**, CP16 displayed a confluence dependent increase in these compartments **(Figure 6. B,D,F).** However, the expression of nuclear p53 in both cell lines was inconsistent across three biological replicates, hence a statistically significant difference could not be observed **(Figure 6. G,H).**

The confluence dependent decrease of cytoplasmic p53 observed in A2780 may indicate that cytoplasmic p53 may become prone to degradation by MDM2 at higher confluency. As for CP16, the confluence dependent increase in cytoplasmic p53 expression may suggest elevated protein stability at higher confluency levels. Moreover, the lack of consistent nuclear p53 expression combined with the cytoplasmic p53 pattern observed in CP16 may imply cytoplasmic sequestration of p53. Altogether, the data highlights that cell confluence has an effect on p53 expression especially in the cytoplasm in response to cisplatin. Moreover, the direction of the confluence dependent change in cytoplasmic p53 in response to cisplatin was opposite in the two cell models, decreasing in parental cell line A2780 and increasing in the cisplatin resistant counterpart CP16.

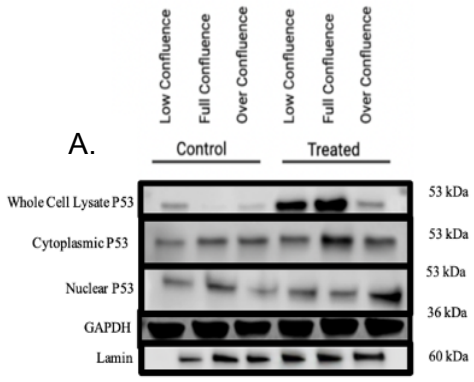

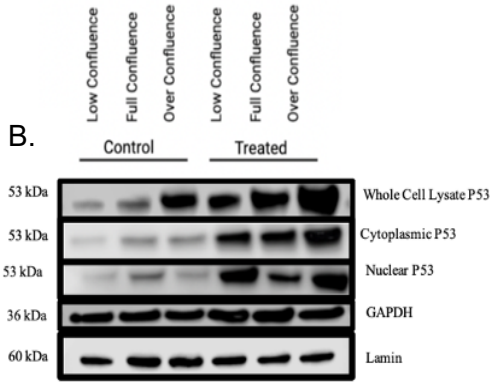

C. Expression of p53 in A2780

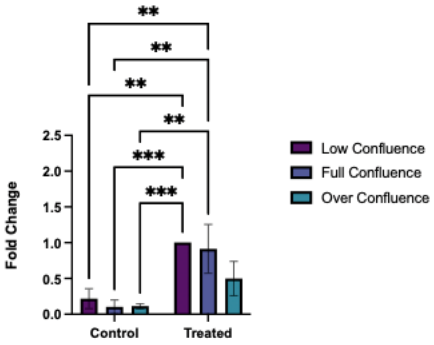

D. Expression of p53 in CP16

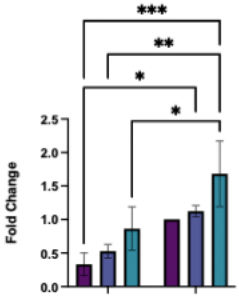

E. Expression of Cytoplasmic p53 in A2780

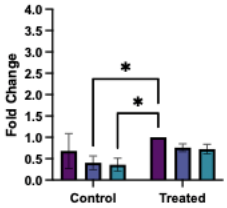

F. Expression of Cytoplasmic p53 in CP16

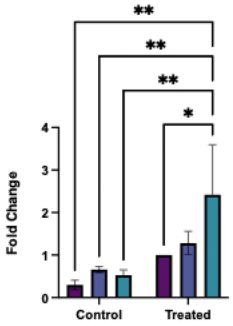

G. Expression of Nuclear p53 in A2780

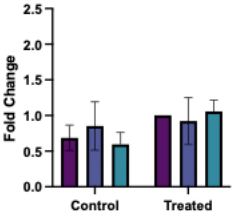

H. Expression of Nuclear p53 in CP16

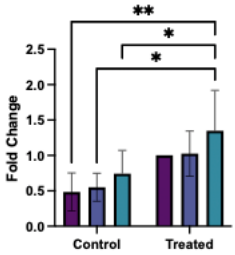

Figure 6: Subcellular expression of p53 in A2780 and CP16 under different confluency levels and in response to cisplatin. Representative western blot images showing whole cell lysate, cytoplasmic and nuclear fractions in A2780 **(A**) and CP16 **(B).** Cells were seeded at low confluent (25%), full confluent (90-100%), and overconfluent (>100%) levels and treated with 1uM (A2780) and 10uM (CP16) of cisplatin respectively for 24 hours. Densiometric analysis of whole cell lysate, cytoplasmic and nuclear p53 in A2780 **(C,E,G)** and CP16 **(D,F,H)**, were normalized to GAPDH (whole cell lysate and cytoplasmic fraction) or Lamin (nuclear fraction) and fold changes in expression with respect to low confluence treated group were calculated. Data represents mean ± standard deviation of three biological replicates. Statistical significance was determined using Two-way Anova. p< *0.05 (*), p* < 0.01 (**), and *p* < 0.001 (***).

3.2.2 Phosphorylated P53 Protein Expression Analysis by Western Blot

To further investigate the effect of confluence on p53 function, western blotting was performed to detect the phosphorylation level of four p53 phosphorylation sites. These sites included two N-terminal sites, Serine 15 and Serine 20, which are responsible for stabilizing P53 and regulating its function as a transcription factor. In addition, the two other phosphorylation sites at the C-terminal, Serine 315 and Serine 392, which regulate nuclear localization and tetramerization of p53 respectively were also assessed (Hafner et al., 2019).

In A2780, serine 15 and 20 residues showed a confluence dependent decrease in phosphorylation **(Figure 7.C,E**) while an opposite pattern was observed in CP16 **(Figure 7.D,F).** These results suggest that the stability of p53 is elevated at higher confluency level in CP16 but decrease in A2780. However, it is unclear whether the transactivation function of p53 in the nucleus is being elevated or reduced by Serine 15 and Serine 20 expression since nuclear p53 expression did not increase respectively.

In regards to, C-terminal phosphorylation sites, serine 315 phosphorylation could be observed consistently in A2780 cells, and it exhibited only a slight and statistically insignificant decrease with increasing confluence in this cell model **(Figure 7. G).** On the other hand, serine 392 phosphorylation of p53 could be observed consistently only in CP16 cells and it displayed a significant confluence dependent increase in phosphorylation in CP16 cells **(Figure 7.J).** Tetramer formation

mediated by serine 392 has been shown to mask the nuclear export signal found in the oligomerization domain of p53, resulting in nuclear retention of the protein (O'Brate & Giannakakou, 2003). Therefore, the confluence dependent increase in the phosphorylation of serine 392 in CP16 would be expected to increase intranuclear p53 expression.

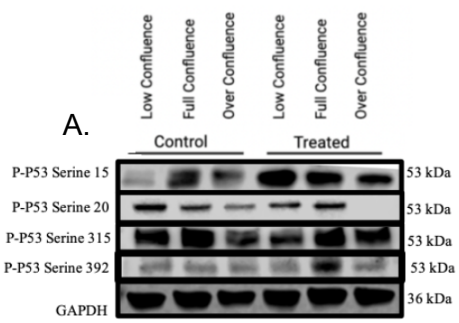

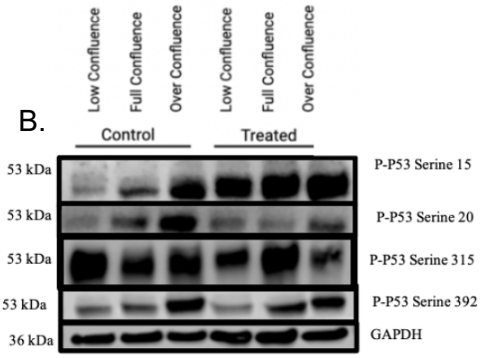

C. Expression of p-p53 Serine 15 in A2780

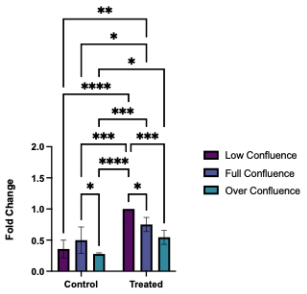

D. Expression of p-p53 Serine 15 in CP16

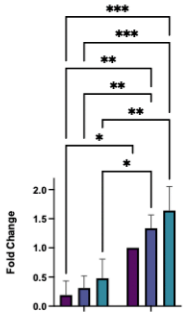

E. Expression of p-p53 Serine 20 in A2780

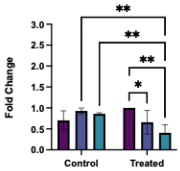

F. Expression of p-p53 Serine 20 in CP16

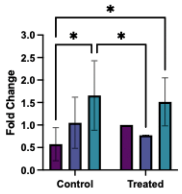

G. Expression of p-p53 Serine 315 in A2780

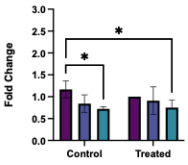

H. Expression of p-p53 Serine 315 in CP16

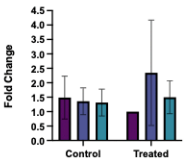

J. Expression of p-p53 Serine 392 in CP16

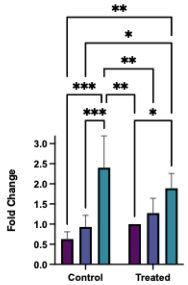

I. Expression of p-p53 Serine 392 in A2780

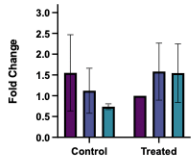

Figure 7: The expression of phosphorylated P53 at Serine-15, Serine 20, Serine-315, and Serine-392 in A2780 and CP16 under different confluency levels and in response to cisplatin. Representative western blot images showing Serine-15, Serine 20, Serine-315, and Serine-392 in A2780 **(A)** and CP16 **(B).** Cells were seeded at low confluent (25%), full confluent (90-100%), and overconfluent (>100%) levels and treated with 1uM and 10uM of cisplatin respectively for 24 hours. Densiometric analysis of P-53 at Serine-15, Serine 20, Serine-315, and Serine-392 in A2780 **(C,E,G,I)** and P-53 at Serine-15, Serine 20, Serine-15 ,and Serine-392 in CP16 **(D,F,H,J),** were normalized to GAPDH and expressed relative to low confluence treated group. Data represents mean ± standard deviation of three biological replicates. Statistical significance was determined using Two-way Anova. p< *0.05 (*), p* < 0.01 (**), and *p* < 0.001 (***).

3.2.3 qPCR Analysis of P53 mRNA Expression

Upon observing that P53 expressed a confluence dependent pattern at the subcellular localization level and in its phosphorylated forms, we assessed whether this phenomenon was solely due to regulation at the post-translational level or also occurs on an mRNA level using qPCR. Our results showed that TP53 expression at the mRNA level does not exhibit a confluence dependent pattern in both A2780 **(Figure 8. A)** and CP16 (**Figure 8. B)** cell lines. However, while the expression of TP53 throughout biological replicates were non consistent in both cell lines, A2780 displayed more pronounced changes in TP53 expression after cisplatin treatment when compared to CP16. Therefore, despite that A2780 TP53 mRNA expression is not regulated in a confluence dependent manner , the response to cisplatin induced damage seems to be more robust in A2780 when compared to CP16. Overall, this data suggests that modifications on the protein level may be the key regulators of the confluence dependent response of p53 to cisplatin in both A2780 and CP16.

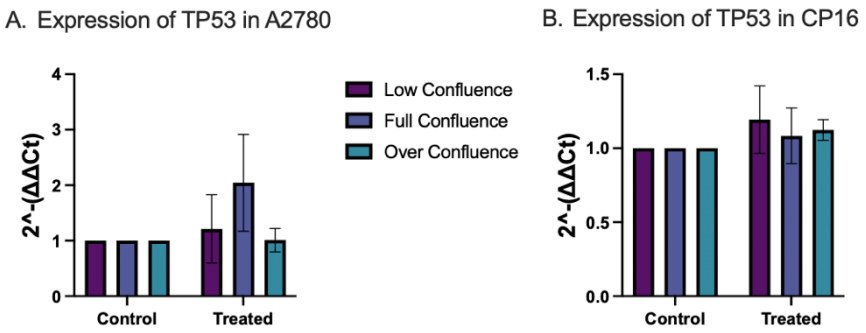

Figure 8: mRNA expression levels of TP53 in A2780 and CP16 cells under different confluency levels and in response to cisplatin. Relative TP53 mRNA expression in A2780 **(A)** and CP16 **(B)**. Cells were seeded at low confluent (25%), full confluent (90-100%), and overconfluent (>100%) levels and treated with 1uM and 10uM of cisplatin respectively for 24 hours. Expression levels were normalized against GAPDH. Data represents mean ± standard deviation of three biological replicates. Fold changes were calculated using the ΔΔCt method. Statistical significance was determined using Two-way Anova. p< *0.05 (*), p* < 0.01 (**), and *p* < 0.001 (***).

3.3 *qPCR Analysis of ATM and ATR analysis in accordance with Cellular Confluency*

ATM and ATR are the two main kinases responsible for the phosphorylation of p53 at Serine 15 and Serine 20 (Smith et al., 2020). Despite not observing a confluence dependent pattern of TP53 expression on the mRNA level, we still considered the possibility that the mRNA expression of the upstream kinases may be regulated in a density dependent manner. However, as shown in **(Figure 9. A,B,C,D)**, the kinases lacked any confluence dependent response to cisplatin in both cell lines. However, similarly to the mRNA expression of TP53, the changes in ATM and ATR levels in A2780 upon exposure to cisplatin were more pronounced than in CP16. Therefore, this data suggests that in addition to TP53, DNA damage response elements upstream of p53 seem to display a more intact response at the mRNA level. However, whether ATM and ATR are being regulated on a protein level in confluence dependent manner is a subject that requires further investigation in future projects.

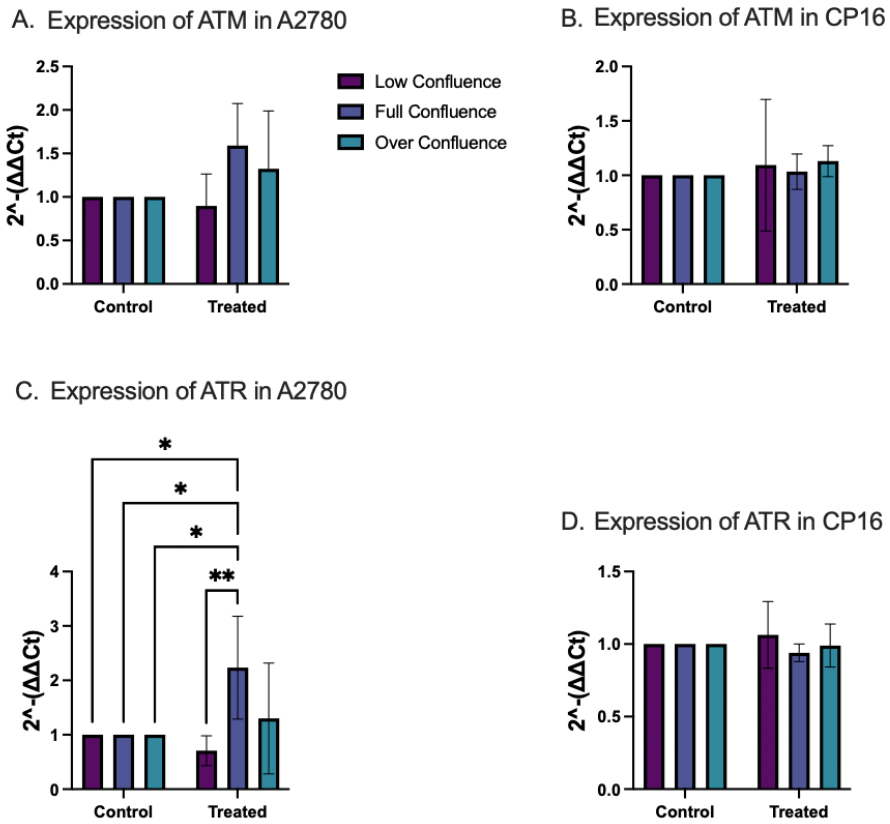

Figure 9: mRNA Expression of ATM and ATR in in A2780 and CP16 under different confluency levels and in response to cisplatin. Relative ATM mRNA expression in A2780 **(A)** and CP16 **(B).** Relative ATR mRNA expression in A2780 **(C)** and CP16 **(D)**. Cells were seeded at low confluent (25%), full confluent (90-100%), and overconfluent (>100%) levels and treated with 1uM and 10uM of cisplatin respectively for 24 hours. Expression levels were normalized against GAPDH. Data represents mean ± standard deviation of three biological replicates. Fold changes were calculated using the ΔΔCt method. Statistical significance was determined using Two-way Anova. p< *0.05 (*), p* < 0.01 (**), and *p* < 0.001 (***).

3.4 *Differential Expression of p21 in Accordance with Cellular Confluency*

3.4.1 Subcellular P21 Protein Expression Analysis by Western Blot

P21 is one of the downstream targets of p53 which is activated to induce cell cycle arrest, DNA repair, or cellular senescence (Karimian et al., 2016) . Studies have shown that nuclear p21 is typically associated with cell cycle arrest, DNA

repair, and proapoptotic functions while cytoplasmic p21 has been linked to oncogenic and antiapoptotic roles as well as being degraded in this compartment (Y. S. Jung et al., 2010) Al Bitar & Gali-Muhtasib, 2019)(Cmielova & Rezacova, 2011).Therefore, in order to understand which function p53 may be inducing through p21 we assessed the expression of the p21 on a subcellular localization level **(Figure 10. A,B)**.

As shown in **(Figure 10. C, D),** whole cell lysate p21 expression is increasing with confluence in both cell lines and in response to both confluence and cisplatin treatment. However, in A2780, p21 expression seems to increase more prominently in response to cisplatin **(Figure 10.C**) when compared to CP16 **(Figure 10.D)**. Although the most prominent expression of p21 was in the nucleus in both cells with a much lower p21 signal in the cytoplasm, the cytoplasmic p21 seem to increase substantially in the overconfluent state in untreated A2780 and CP16 cells **(Figure 10. E,F)**, despite that there is no statistical significance due to high variability in biological replicates. Furthermore, our data revealed a slight but statistically insignificant confluence dependent nuclear p21 increase in A2780 **(Figure 10. G)** while the levels were inconsistent in CP16 **(Figure 10. H)**. Based on this data, we hypothesized that increase in p21 may contribute to the confluence dependent increase in cisplatin resistance in both cell lines. However, whether cytoplasmic p21 or nuclear p21 contribute to this process could not be discerned based on the present data.

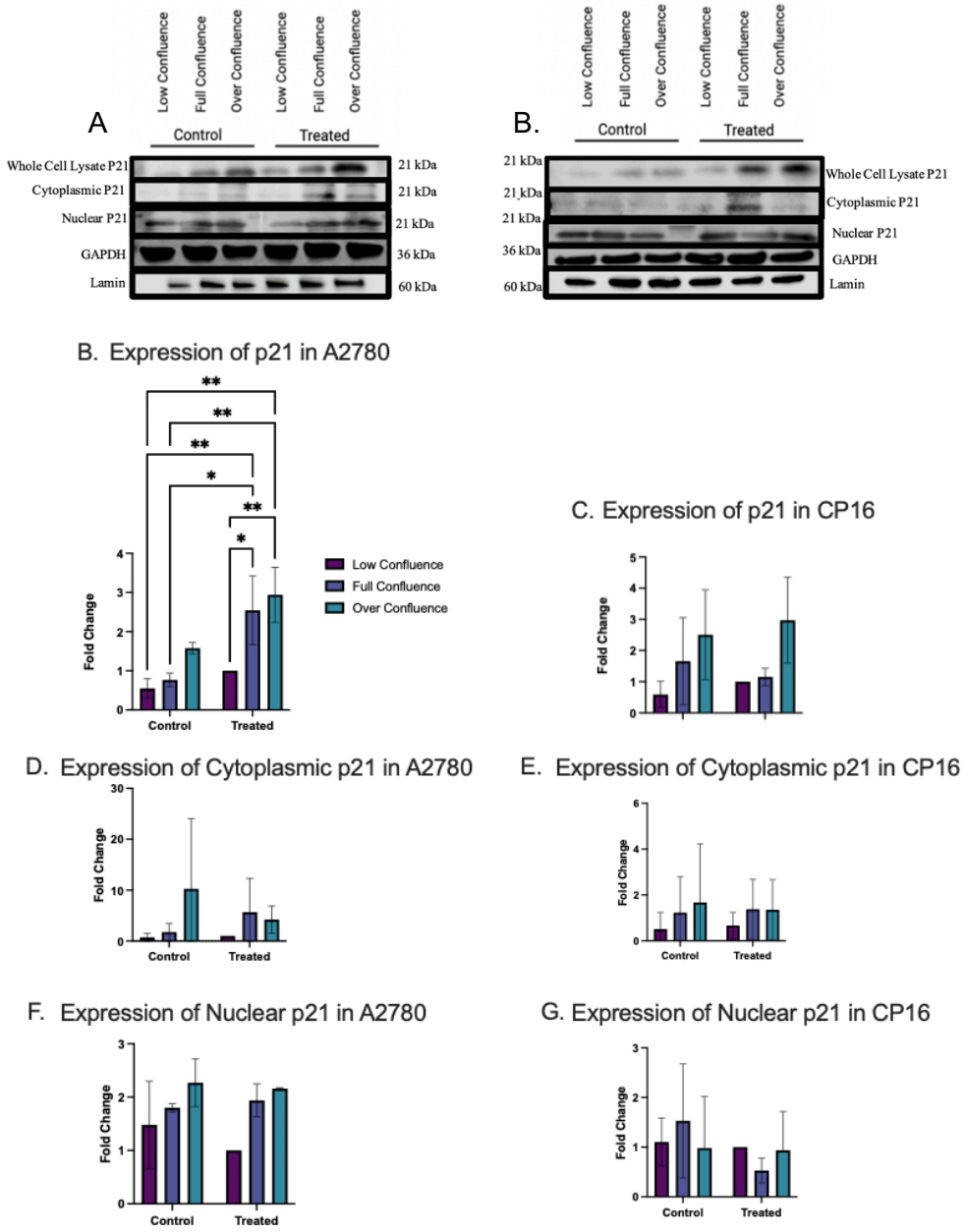

Figure 10: Subcellular expression of p21 in A2780 and CP16 under different confluency levels and in response to cisplatin. Representative western blot images showing whole cell lysate, cytoplasmic and nuclear fractions in A2780 **(A**) and CP16 **(B).** Cells were seeded at low confluent (25%), full confluent (90-100%), and overconfluent levels (>100%) and treated with 1uM and 10uM of cisplatin respectively for 24 hours. Densiometric analysis of whole cell lysate, cytoplasmic and nuclear p21 in A2780 **(C,E,G)** and CP16 **(D,F,H)** were normalized to GAPDH (whole cell lysate and cytoplasmic fractions) or Lamin (nuclear fractions) and expressed relative to the low confluence treated group. Data represents mean ± standard deviation of three biological replicates. Statistical significance was determined using Two-way Anova. p< *0.05 (*), p* < 0.01 (**), and *p* < 0.001 (***).

3.4.2 Phosphorylated P21 Protein Expression Analysis by Western Blot

To verify the results obtained from the p21 subcellular localization expression, we investigated the phosphorylation level of p21 sites, threonine-145 and serine-146 which are associated with cytoplasmic localization (Abbas & Dutta, 2009) **(Figure 11.A,B).** We observed confluence dependent increases in Threonine 145 and Serine 146 phosphorylation of p21 in both cell lines but only in response to cisplatin (**Figure 11.C,D,E,F).** But this increase was statistically insignificant due to high variation between biological replicates. Therefore, an interpretation on whether phosphorylation of p21 at threonine-145 and serine-146 can contribute to cell-density dependent cisplatin resistance could not be made with the current data.

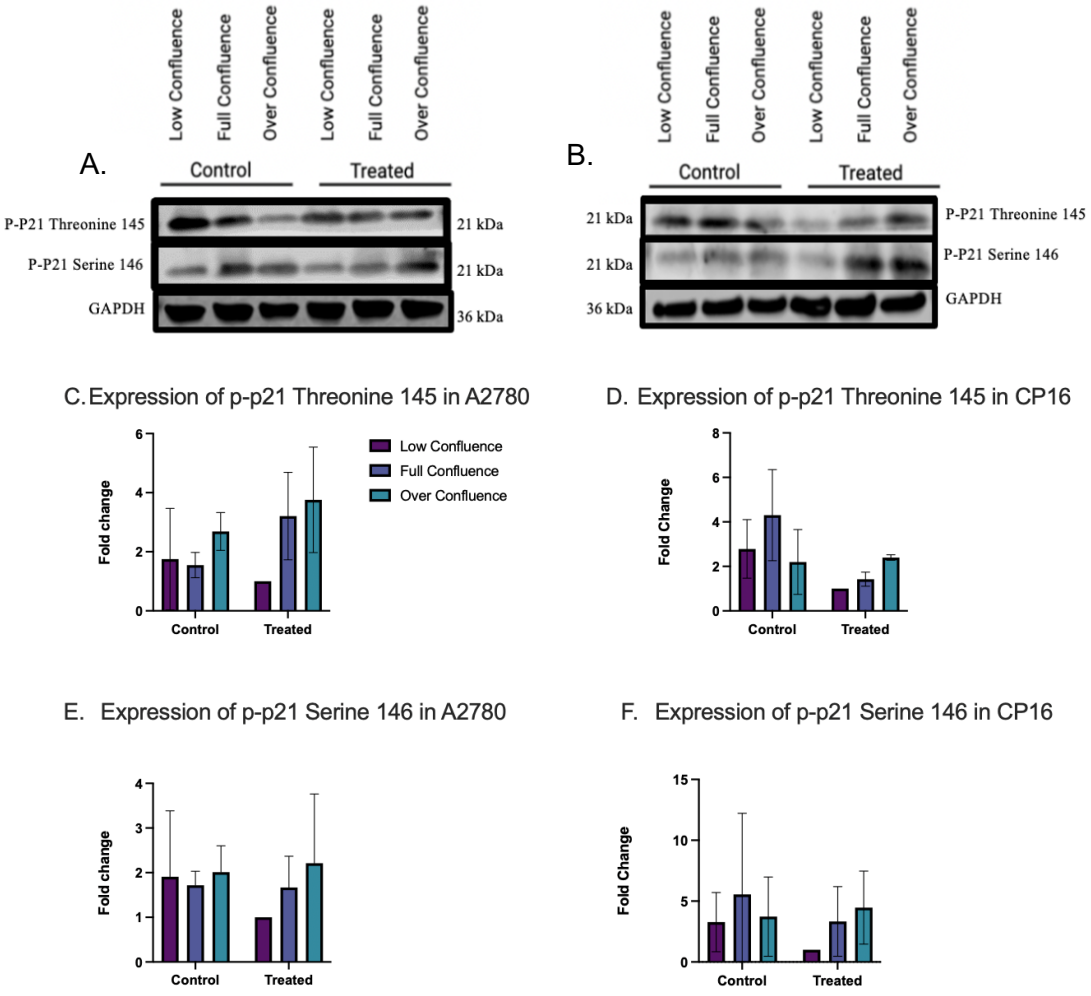

Figure 11: The expression of phosphorylated p21 at Threonine-145 and Serine-146 in A2780 and CP16 under different confluency levels and in response to cisplatin. Representative western blot images showing P-P21threonine-145 and terine-146 in A2780 **(A)** and CP16 **(B)**. Cells were seeded at low confluent, full confluent, and treated with 1uM and 10uM of cisplatin respectively for 24 hours. Densiometric analysis of P-P21 threonine-145 and serine-146 in A2780 **(C,E)** and CP16 **(D,F),** normalized to GAPDH and expressed relative to low confluence treated group. Data represents mean ± standard deviation of three biological replicates. Statistical significance was determined using Two-way Anova. p< *0.05 (*), p* < 0.01 (**), and *p* < 0.001 (***).

3.4.3 qPCR Analysis of p21 mRNA Expression

As a result of observing a confluence dependent pattern expression of p21 at a protein level, we investigated whether a similar pattern is observed on an mRNA level. Similarly to p53, mRNA expression of p21 was inconsistent across three biological replicates and the results did not display a confluence dependent pattern. **(Figure *12*. A,B).** However, upon exposure to cisplatin, p21 is activated at higher levels in CP16 when compared to A2780, in contrary to the findings at the protein level **(Figure 10.A-D)** This data suggests that similar to TP53, modifications on the protein level may be the key regulators of confluence dependent response of p21 to cisplatin in both A2780 and CP16.

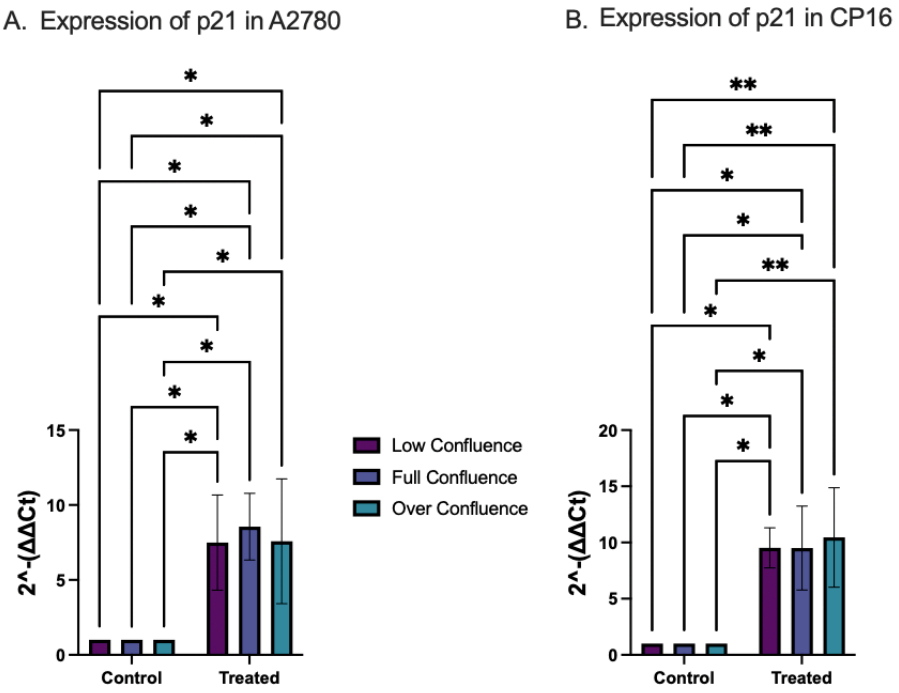

Figure 12: mRNA expression levels of p21 in A2780 and CP16 cells under different confluency levels and in response to cisplatin. Relative p21 mRNA expression in A2780 **(A)** and CP16 **(B).** Cells were seeded at low confluent (25%), full confluent (90-100%), and overconfluent (>100%) treated with 1uM and 10uM of cisplatin respectively for 24 hours. Expression levels were normalized against GAPDH. Data represents mean ± standard deviation of three biological replicates. Fold changes were calculated using the ΔΔCt method. Statistical significance was determined using Two-way Anova. p< *0.05 (*), p* < 0.01 (**), and *p* < 0.001 (***).

3.5 *The Confluence Dependent Differential Regulation of DNA Damage and Apoptosis Markers in Response to Cisplatin*

As previously mentioned, p53 is able to induce apoptosis through the intrinsic apoptotic pathway in response to DNA damage. However, p53 is also able to induce extrinsic apoptosis through the Fas/FasL receptor (Galluzzi et al., 2018). Therefore, we continued to investigate ɣ-H2AX as a double stranded DNA break marker and apoptotic pathway components including caspase-9 and its cleaved form as an indicator of intrinsic apoptosis, caspase-8 and its cleaved form as an indicator of extrinsic apoptosis, and caspase-3 and its cleaved form as the final apoptotic executioner of both apoptotic pathways (**Figure 13.A,B).**

Figure *13*.C displays the expression of ɣ-H2AX in A2780 which interestingly increases with confluence in response to cisplatin. In regards to CP16, more interestingly, a confluence dependent increase in ɣ-H2AX is observed in both control and cisplatin treated conditions, indicating possible baseline confluence dependent genomic instability (**Figure 13.D)**. Moreover, in response to cisplatin, the increase of ɣ-H2AX levels in CP16 seems to be minimal. This may be due to decreased DNA damage or increased DNA repair in CP16 cells. However, which mechanisms would explain the increase in DNA damage with increasing cell density are unclear.

As for the intrinsic apoptotic pathway, A2780 exhibited a confluence dependent expression of both caspase 9 and its cleaved form, indicating intact execution of upstream intrinsic apoptosis (**Figure 13.E,G)**. On the other hand, CP16 only exhibited a confluence dependent expression of caspase-9 under control conditions but no change in treated group. Cleaved caspase -9 under control conditions and in response to cisplatin was inconsistent and lacked any confluence dependent expression in CP16 (**Figure 13.F,H)**. This suggests nonfunctional intrinsic apoptosis in CP16 cells. A possible explanation can be p53 mediated inhibition of cleaved caspase-9 which is an occurrence that has been observed in ovarian cancer cells (Chee et al., 2013).

In regards to extrinsic apoptosis, caspase-8 did not exhibit any change with increasing confluence in A2780 cells (**Figure *13*.I)**, but its cleaved form increased as confluence increases (**Figure *13*.K)**. This indicated that intrinsic apoptosis may also contribute to cell death in A2780 cells. On the contrary, while full length caspase-8 exhibited a confluence dependent increase in CP16 cells (**Figure *13*.J)**. The expression cleaved caspase-8 was inconsistent and very low in response to cisplatin, therefore, densiometric analysis of cleaved caspase-8 was not presented, since the bands could not be observed in most of the samples**.** These data indicated that there may be a resistance to apoptosis at both extrinsic and intrinsic pathways in CP16.Finally, assessment of executioner caspase-3 (**Figure *13*. L)** and its cleaved

form in A2780 (**Figure 13.N)** showed a confluence dependent increase in both forms as expected**.** However, in CP16 cells no statistically significant increase in full length and cleaved caspase-3 could be observed, despite that caspase -3 and cleaved caspase-3 expression showed a confluence dependent pattern (a slight decrease for caspase-3 and a slight increase for cleaved caspase-3) **(Figure 13.M,O)**.

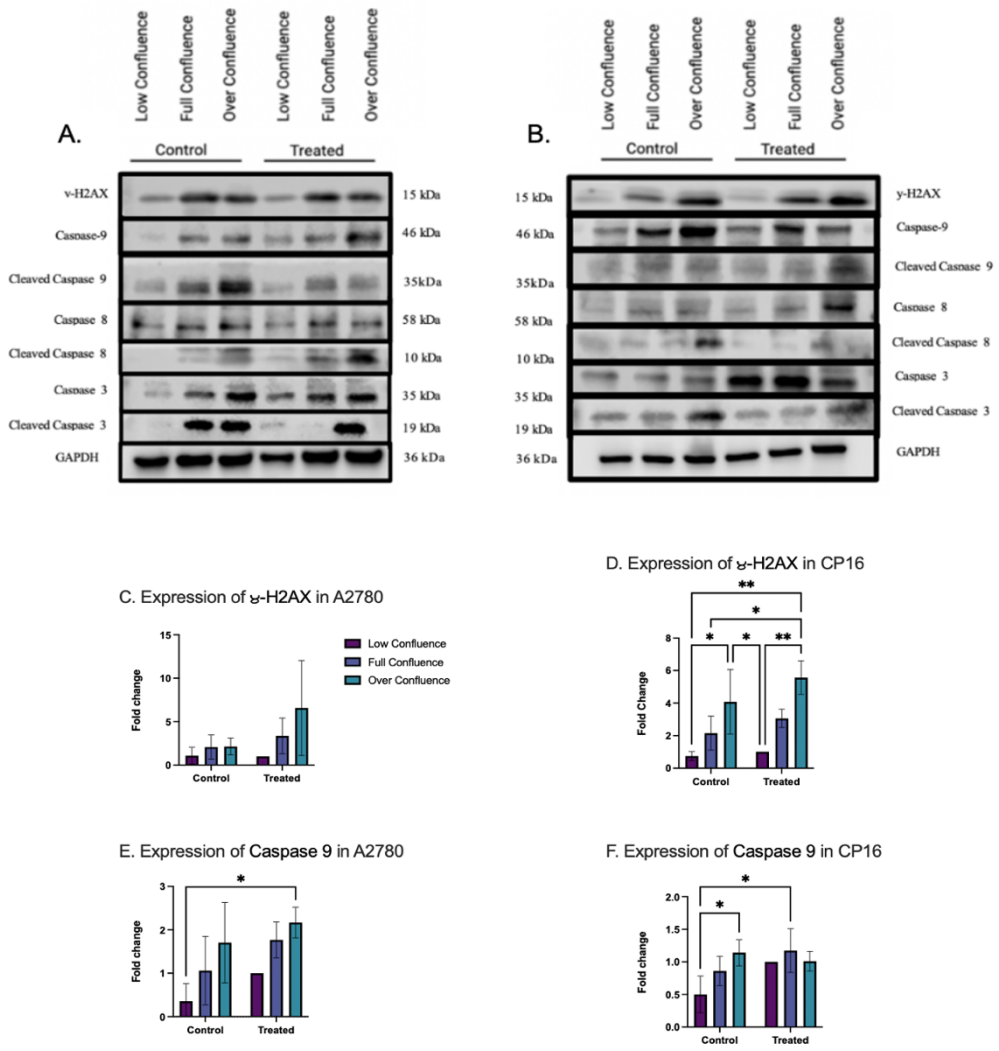

G. Expression of Cleaved Caspase 9 in A2780

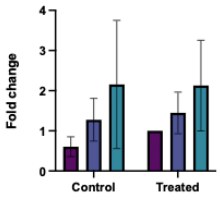

H. Expression of Cleaved Caspase 9 in CP16

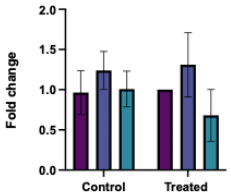

I. Expression of Caspase 8 in A2780

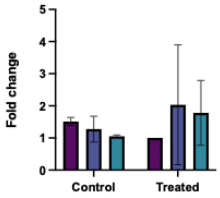

J. Expression of Caspase 8 in CP16

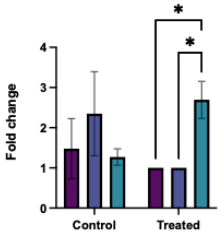

K. Expression of Cleaved Caspase 8 in A2780

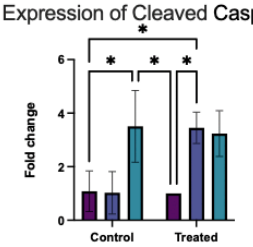

L. Expression of Caspase 3 in A2780

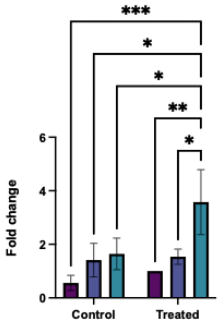

M. Expression of Caspase 3 in CP16

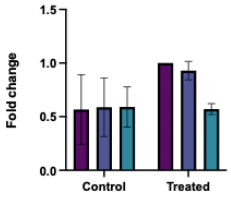

N. Expression of Cleaved Caspase 8 in A2780

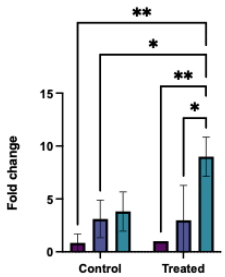

O.Expression of Cleaved Caspase 3 in CP16

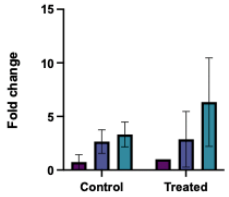

Figure 13: The expression of apoptotic components in A2780 and CP16 under different confluency levels and in response to cisplatin. Representative western blot images showing ɣ-h2ax, 9, cleaved caspase-9, caspase-8, cleaved caspase-8, Caspase-3 and cleaved caspase 3 in A2780 **(A)** and CP16 **(B**) Cells were seeded at low confluent (25%), full confluent (90-100%), and overconfluent (>100%) levels treated with 1uM and 10uM of cisplatin respectively for 24 hours. Densiometric analysis of y-h2ax, caspase-9, cleaved caspase-9, caspase-8, cleaved caspase-8, caspase-3 and cleaved caspase-3 in A2780 **(C,E,G,I,K,L,N)** and CP16 **(D,F,H,J,M,O)** normalized to GAPDH and expressed relative to low confluence treated group. Data represents mean ± standard deviation of three biological replicates. Statistical significance was determined using Two-way Anova. p< *0.05 (*), p* < 0.01 (**), and *p* < 0.001 (***). Densiometric analysis of cleaved caspase-8 was not included as bands were only observed in one biological replicate.

3.5.1 *Validation of Apoptosis*

Lamin B1 cleavage

Studies have shown that despite the expression of active caspases within apoptotic pathways, mutations may occur at the level of apoptosis which could prevent the execution of apoptosis or delay it (Ghavami et al., 2009). Therefore, we further investigated the apoptotic marker, Lamin B1 which is cleaved downstream of executioner caspase-3. As shown in **(Figure 14.A)** Cleaved Lamin B1 bands are present in all A2780 confluency groups, indicating the occurrence of apoptosis in response to both confluence and cisplatin mediated stress. On the other hand, CP16 did not express cleaved of Lamin B1 under any condition which suggests that apoptosis is not taking place **(Figure 14.B)** Furthermore, densiometric analysis of Cleaved Lamin B1/ Lamin B1 **(Figure 14.C)** revealed that apoptosis is occurring in a density dependent manner in A2780 cells in which higher density groups displayed higher levels of apoptosis. Due to the lack of cleaved Lamin B1 in CP16, we hypothesize that apoptosis may be delayed, or cell death may be executed through other forms.

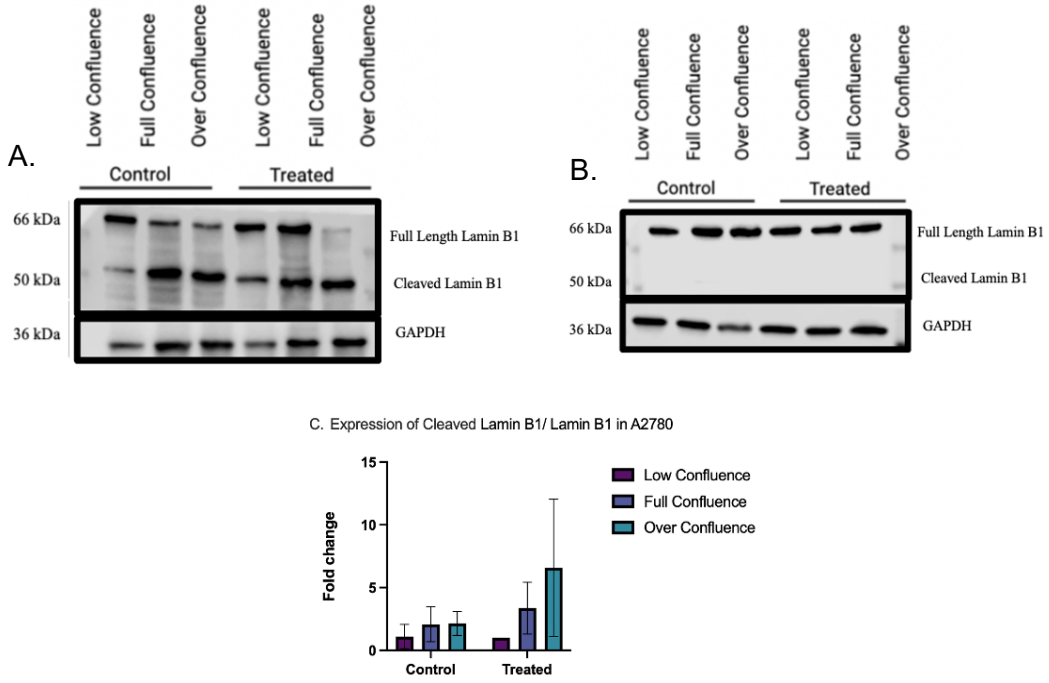

Figure 14: The expression of Lamin B1 and Cleaved Lamin B1 in A2780 and CP16 under different confluency levels and in response to cisplatin. Representative western blot images showing Lamin B1 and cleaved Lamin B1 in A2780 **(A)** and CP16 **(B)** Low confluent (25%), full confluent (90-100%), and overconfluent (>100%) and treated with 1uM and 10uM of cisplatin respectively for 24 hours. **(C)** Densiometric analysis of Cleaved Lamin B1/ Full length Lamin B1 in A2780. normalized to GAPDH and expressed relative to low confluence treated group. Data represents mean ± standard deviation of three biological replicates. Statistical significance was determined using Two-way Anova. p< *0.05 (*), p* < 0.01 (**), and *p* < 0.001 (***).

Annexin V

To further investigate the mechanisms of apoptotic execution, we assessed annexin V expression using the MUSE cell analyzer. However, as we didn't observe cleaved Lamin B1 in CP16 after 24 hours of treatment, we increased cisplatin exposure to 3 days. As shown in **Figure 15. A** below, A2780 cell did not express a significant change in Annexin V expression across different confluence groups. However, CP16 cells exhibited a significant downregulation of annexin V expression with increasing confluence levels (**Figure 15. B).** In comparison to cleaved Lamin B1 expression in A2780, annexin V expression may indicate that an

increase in cisplatin exposure leads to the loss of the confluence dependent apoptotic response. On the other hand, in CP16, the expression of annexin V as an apoptotic indicator only after 3 days of treatment indicates a possible delay in apoptotic execution. Additionally, the observed confluence dependent decrease in annexin V expression aligns with our MTT results which indicates increased resistance at higher confluence groups due to a block in apoptotic execution.

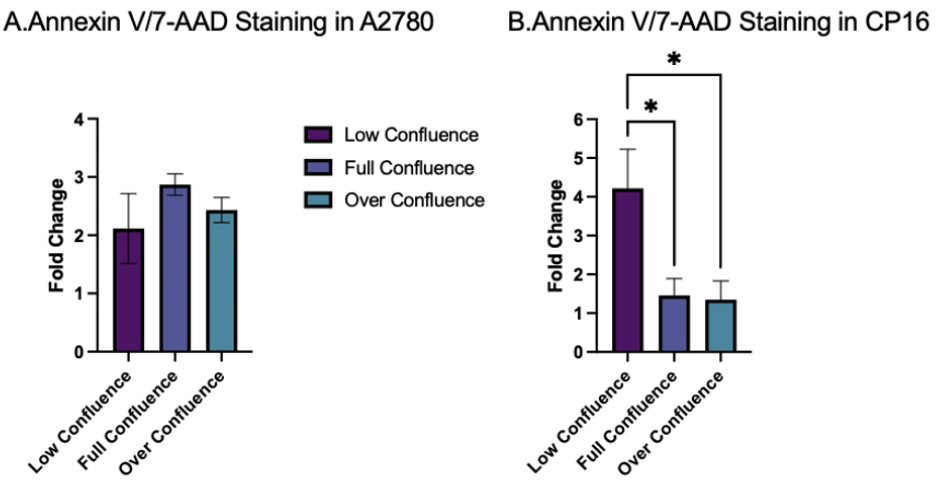

Figure 15: Annexin V-fold change levels in A2780 and CP16 cells under different confluency levels in response to cisplatin treatment. Analysis of Annexin Fold change in A2780 **(A)** and CP16 **(B)** Low confluent (25%), full confluent (90-100%), and overconfluent (>100%) groups and treated with 1uM and 10uM of cisplatin respectively for 3 days. Data represents mean ± standard deviation of two biological replicates. Statistical significance was determined using One-way Anova. p< *0.05 (*), p* < 0.01 (**), and *p* < 0.001 (***).

3.6 *Confluency-Dependent Expression of Cisplatin Transporters CTR1, CTR2, ATP7A, and ATP7B*

After confirming the role of a number of cell signaling pathways in the confluence dependent response to cisplatin, we wondered whether cisplatin transporters expressed a similar pattern. Initially we investigated the protein expression of CTR1, however, we were unable to validate the accuracy of CTR1 antibodies ordered from 3 different producers. Therefore, we continued to investigate the mRNA expression

of cisplatin uptake transporters CTR1 and CTR2 along with cisplatin efflux pumps, ATP7A and ATP7B using qPCR. In A2780, the expression of CTR2, and ATP7B was inconsistent and lacked a confluence dependent response (**Figure 16. C,G).** On the other hand, ATP7A and CTR1 expression was consistent but the pattern of change was not similar to the one observed in p53 or p21 and did not gradually change with increasing confluence (**Figure 16.A,E).** In this case, ATP7A expression peaked at full confluence and was minimal at the low confluence group. A converse pattern was observed in CTR1 expression; however, minimal expression was observed at the overconfluent group. We hypothesize that a reasoning for that can be in relation to contact inhibition which occurs when cell reach 100% confluency. As for CP16, the expression of CTR2 and ATP7A was inconsistent across three biological replicates **(Figure 16. D,F).** However, CTR1 and ATP7B expression were consistent **(Figure 16. B,H).** Moreover, while ATP7B expression was confluence dependent, CTR1 expressed minimal expression at full confluence which similarly to A2780, may be related to contact inhibition. A confluence dependent decrease in ATP7B expression may suggest confluence dependent increase in cisplatin accumulation in CP16 cells. This would be in line with the density dependent increase in DNA damage in CP16 cells. To test this hypothesis, we are in the process of assessing intracellular cisplatin accumulation through atomic force spectrometer and imaging of quantum-dot labeled cisplatin in live cells.

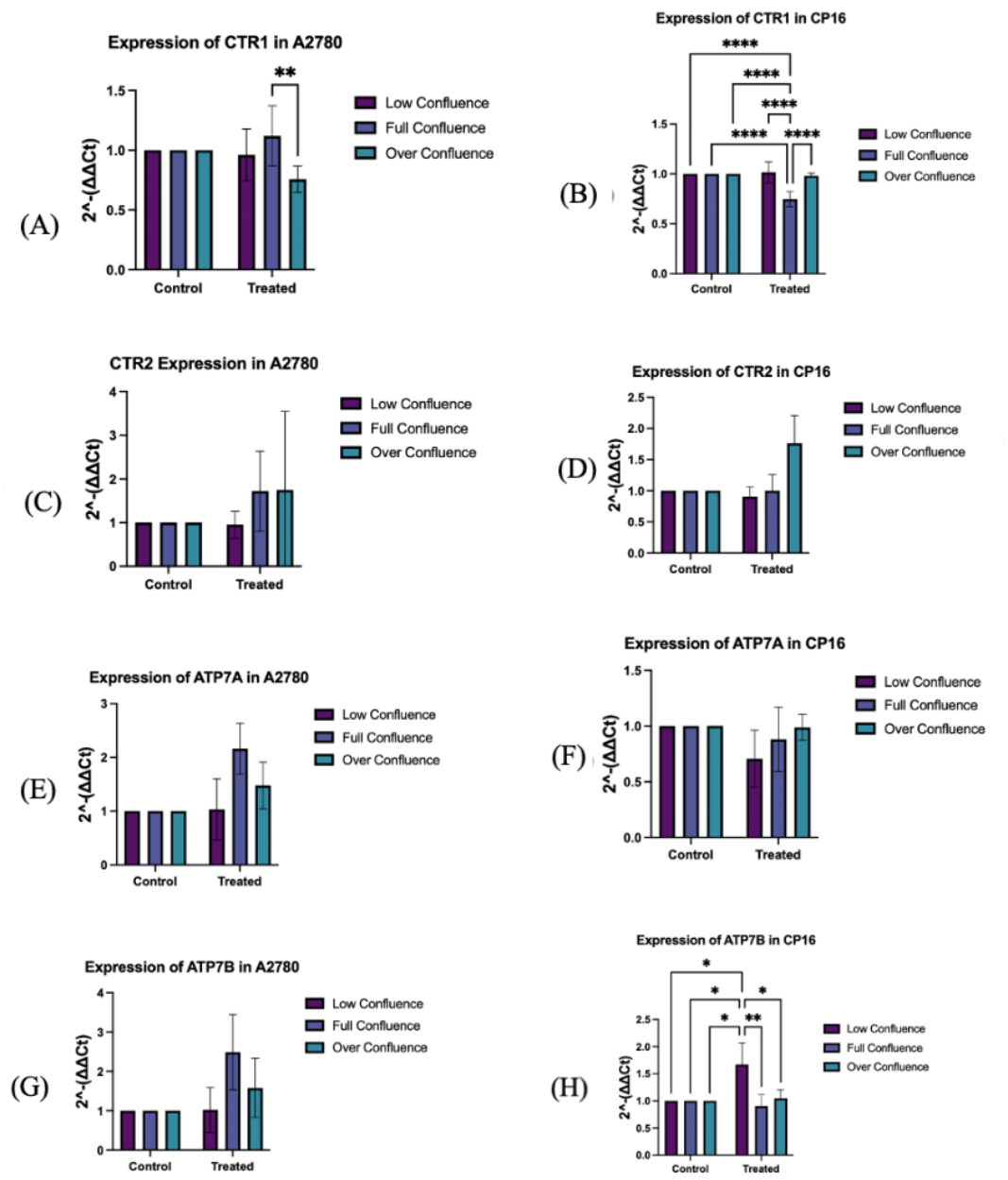

Figure 16: mRNA expression levels of copper transporters in A2780 and CP16 cells under different confluency levels and in response to cisplatin. Relative CTR1,CTR2, ATP7A, and ATP7B mRNA expression in A2780 **(A,C,E,G)** and CP16 **(B,D,F,H).** Cells were seeded at low confluent, full confluent, treated with 1uM and 10uM of cisplatin respectively for 24 hours. Expression levels were normalized against GAPDH. Data represents mean ± standard deviation of three biological replicates. Fold changes were calculated using the ΔΔCt method. Statistical significance was determined using Two-way Anova. p< *0.05 (*), p* < 0.01 (**), and *p* < 0.001 (***).

3.7 *The Effects of Cellular Density at The Time of Treatment to Cisplatin Responses*

The density dependent cisplatin resistance may be due to the cellular state at the time of treatment or differential regulation of signaling mechanisms throughout the exposure to cisplatin. Based on the data which suggests that the expression of drug influx or efflux pumps may be regulated by cell-cell interactions (Wilczyński et al., 2024), we thought that cell density at the time of treatment may lead to confluence dependence in cisplatin responses, since different degrees of cell-cell contact may lead to differences in intracellular cisplatin accumulation. To address this, we treated A2780 and CP16 cells at different confluence levels with cisplatin for 24 hours instead of the 120 hours of treatment protocol we performed in MTT assay. After 24 hours we detached the cells and seeded to 6 well plates at equal numbers to conduct colony formation assay. By this way all groups were incubated at very low confluence levels for 7 days. We could not observe a change in cisplatin concentration-response curves and cisplatin IC50 values neither in A2780 nor CP16 cells **(Figure 17. B,D).** These data suggested that confluence dependent regulation of signaling mechanisms which are responsible for the mechanism of action of cisplatin, may be the underlying cause of density dependent resistance, rather than the confluence at the time of exposure in ovarian cancer cells.

A.

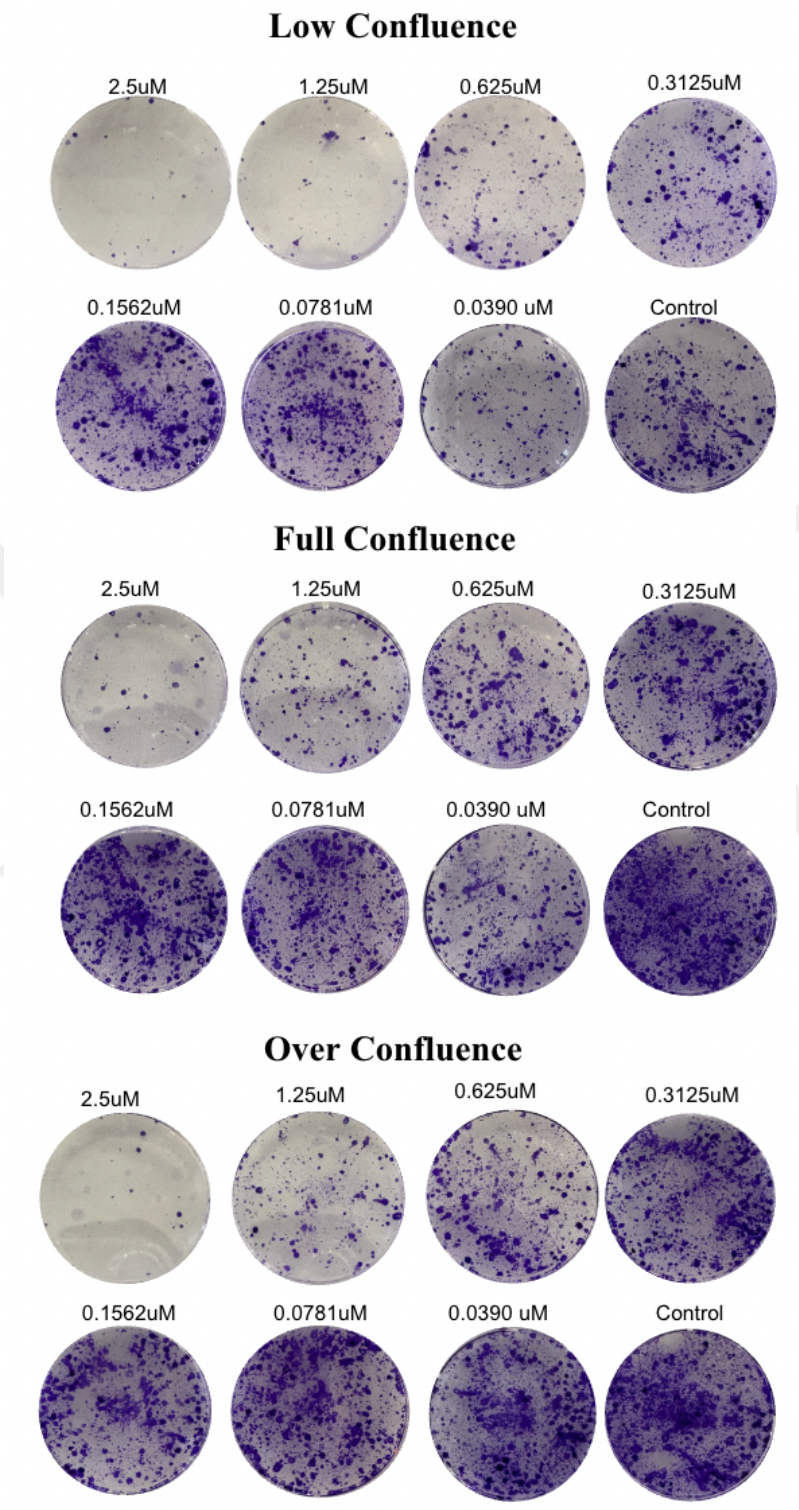
Low Confluence
2.5uM
1.25uM
0.625uM
0.3125uM
0.1562uM
0.0781uM
0.0390 uM
Control
Full Confluence
2.5uM
1.25uM
0.625uM
0.3125uM
0.1562uM
0.0781uM
0.0390 uM
Control
Over Confluence
2.5uM
1.25uM
0.625uM
0.3125uM
0.1562uM
0.0781uM
0.0390 uM
Control

B. **Colony Formation Assay - A2780**

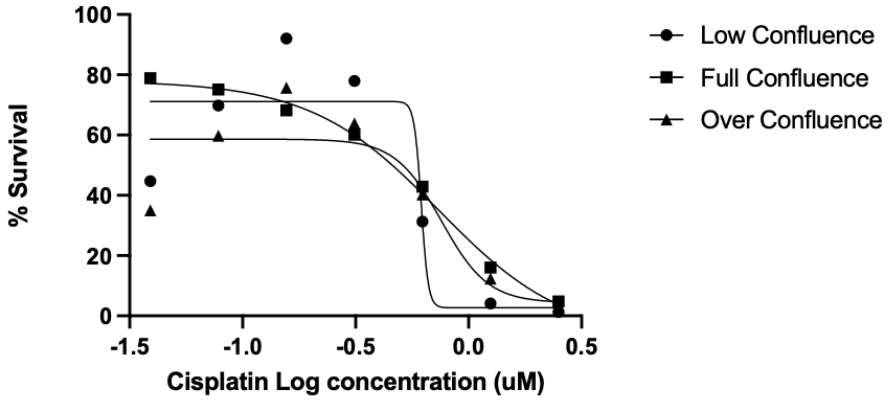

	Low Confluence	Full Confluence	Over Confluence
IC50	0.6176	0.7345	0.7586

C.

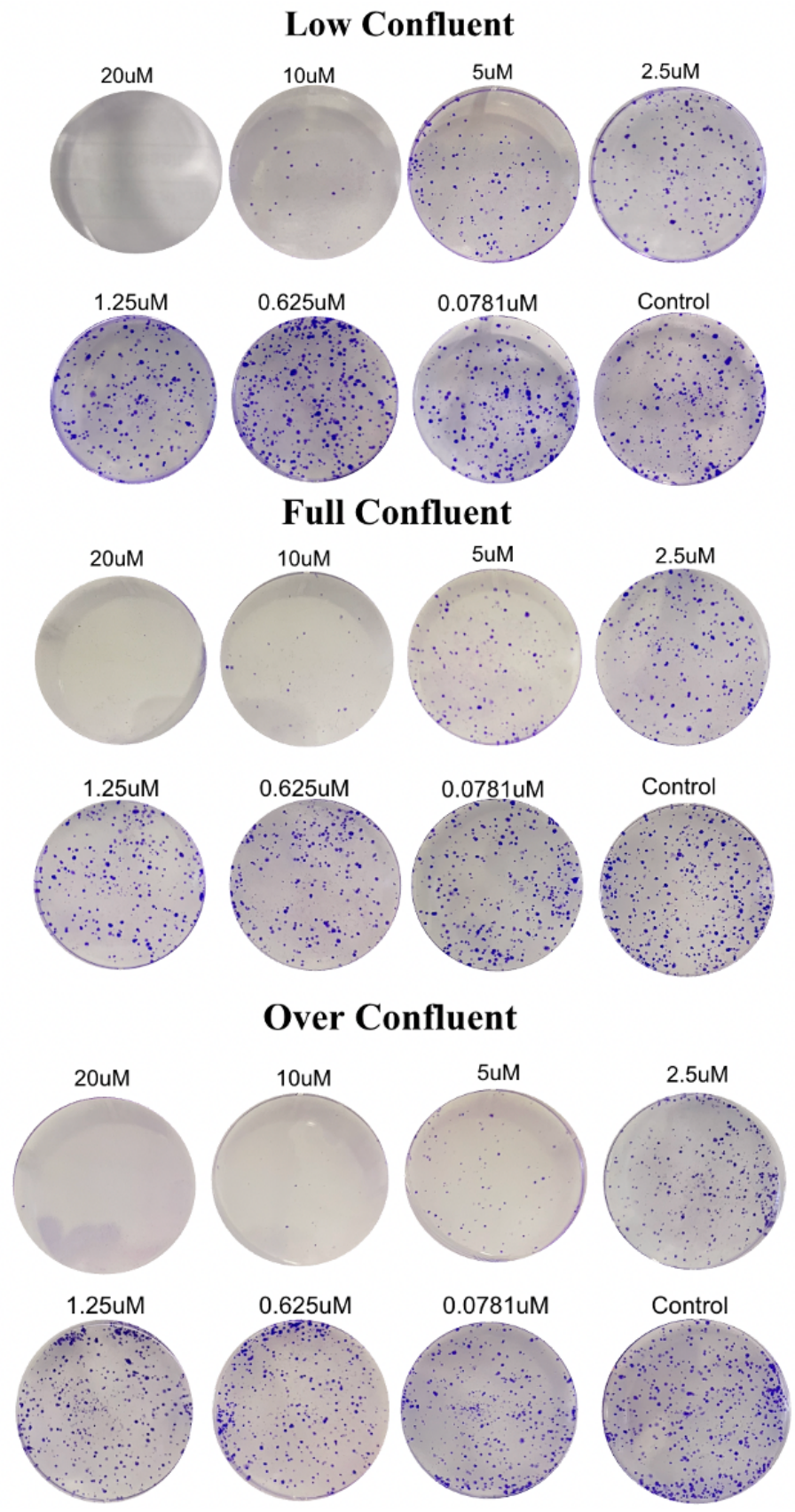
Low Confluent
20uM
10uM
5uM
2.5uM
1.25uM
0.625uM
0.0781uM
Control
Full Confluent
20uM
10uM
5uM
2.5uM
1.25uM
0.625uM
0.0781uM
Control
Over Confluent
20uM
10uM
5uM
2.5uM
1.25uM
0.625uM
0.0781uM
Control

D. **Colony Formation Assay - CP16**

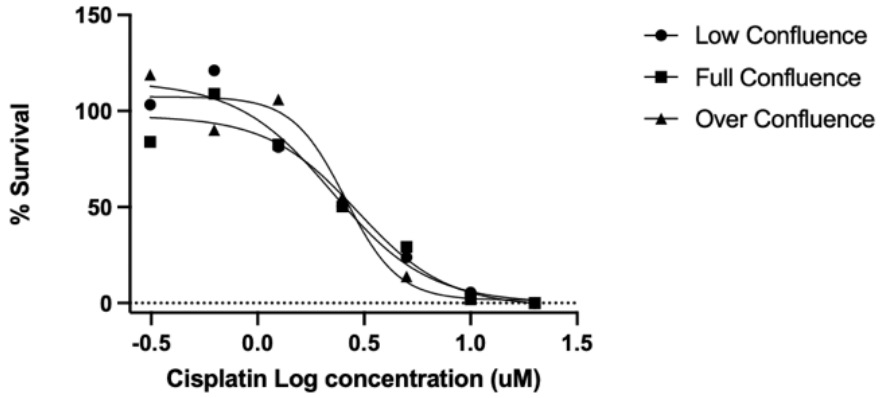

	Low Confluence	Full Confluence	Over Confluence
IC50	2.241	2.938	2.579

Figure 17: Percent survival and IC50 in relation to cellular confluence and colony formation capabilities in A2780 and CP16. Representative images of crystal violet-stained colony formation assay in A2780 **(A)** and CP16 **(C)**. Low confluent (25%), full confluent (90-100%), and overconfluent (>100%) and treated with 1uM and 10uM of cisplatin respectively for 24 hours. Following that, cells very detached are reseeded at equal and low cell seeding density and grown until visible and independent colonies formed. Quantification of percent survival relative to intreated control in A2780 (**B)** and CP16 (**D)**. To calculate the IC50 values, a log (inhibitor) vs response (variable slope) non-linear regression model was used.

In summary, we observed a slight increase in DNA damage with increasing confluence in A2780 cells. This increase was accompanied by a confluence dependent decrease in p53 but increase in p21 in these cells. Although there was also a confluence dependent activation of intrinsic apoptosis pathway in these cells, the cisplatin IC50 values slightly increased in A2780 cells.

On the other hand, we observed a significant and confluence dependent increase in DNA damage in CP16 cells. Despite that this increase was accompanied by a confluent dependent increase in especially cytoplasmic p53 which is expected to perform apoptotic functions, these cells exhibited resistance at the apoptosis level. A

possible non-functionality of cytoplasmic p53 in these cells and an accompanying increase in cytoplasmic p21 which is known to serve antiapoptotic functions may explain the resistance to apoptosis despite high DNA damage in CP16 cells.

Chapter 4:
DISCUSSION

Resistance to cisplatin remains one of the main obstacles preventing its effective usage to treat ovarian cancer patients. A new mechanism of chemotherapeutic resistance was proposed by (He et al., 2016) in which they reported that cell seeding density contributes to differential cisplatin IC50 values in ovarian cancer cell lines. This phenomenon was further confirmed by (Punyamurtula et al., 2023) where they demonstrated a confluence dependent increase in cisplatin IC50 values in a number of cancer cell types. However, the detailed mechanisms that underly cell density dependent cisplatin resistance in ovarian cancer is unknown yet. Therefore, we investigated the role of p53 and p21 in this process, since these molecules are key to the action of cisplatin.

4.1 *The role of p53 localization and phosphorylation in the confluence dependent response to cisplatin*

p53 is one of the main proteins activated after cisplatin induced DNA damage. It plays a key role to determine whether the cell will repair the DNA damage or undergo apoptosis after cisplatin treatment (Siddik, 2003). In this study, we hypothesized that the confluence dependent increase in cisplatin resistance may be modulated by p53 activity, differentially regulated with changing cell densities. Using cisplatin sensitive A2780 and its resistant counterpart CP16 ovarian cancer cell models, we identified a confluence dependent increase in cisplatin IC50 values similar to the recent findings in the literature (Punyamurtula et al., 2023). However, cisplatin resistant CP16 cells exhibited a more prominent confluence dependent increase in IC50 values when compared to A2780 **(Figure 5.C)**. Following that, we assessed the expression and subcellular localization of p53 on a protein level. Studies have shown that in response to cellular stress, p53 accumulates in the nucleus to transactivate stress response elements and increase the expression of p21, GADD45a and PCNA which lead to cell cycle arrest, enabling the cell to repair damaged DNA (Hernandez Borrero & El-Deiry, 2021). The phosphorylation of p53 at N-terminal sites, Serine-15 and Serine-20, reduces the protein's binding affinity to negative regulator MDM2

which also promote nuclear p53 accumulation. On the other hand, cytoplasmic p53 is associated with mitochondrial apoptosis and MDM2-mediated degradation (Green & Kroemer, 2009).

We observed a confluence dependent decrease in overall p53 expression in A2780 **(Figure 6. C)** and a confluence dependent increase in CP16 cells **(Figure 6. D)**. To further understand whether this is due to a change in cytoplasmic or nuclear p53, we investigated nuclear and cytoplasmic p53 expression. Upon observing a decline in cytoplasmic p53 at overconfluent level in A2780 **(Figure *6*.E)** and a lack of respective increase in nuclear p53 levels **(Figure *6*.G)**, we hypothesized that p53 may be degraded in the cytoplasm in A2780 cells. Oppositely, the confluence dependent increase in cytoplasmic p53 **(Figure *6*.F)** and the lack of respective decrease in nuclear p53 **(Figure *6*.H)** indicated increased stability of p53 in CP16 cells. To further validate our hypotheses, we continued to assess p53 phosphorylation sites Serine 15 and Serine 20 **(Figure 7.A,B)**. Our results revealed that both N-terminal phosphorylation sites **(Figure 7.C,D,E,F)** followed the same pattern as cytoplasmic p53 expression **(Figure *6*.E,F)**, decreasing phosphorylation with confluence in A2780 and increasing phosphorylation with confluence in CP16. These results further supported that cytoplasmic p53 in A2780 seems to be degraded at higher confluency levels due to a decline in serine 15 and serine 20 phosphorylation. On the other hand, higher confluency levels seem to stabilize p53 in CP16 cells through increasing serine 15 and serine 20 phosphorylation.

Moreover, we continued to examine C-terminal phosphorylation sites, Serine 315 and Serine 392 due their roles in subcellular localization **(Figure 7.G,H,I,J)** Studies have shown that the serine 315 phosphorylation site lies within a nuclear localization signal region (Dyson & Wright, 2025). As for serine 392, it was shown that the presence of p53 in tetramer form stems from serine 392 phosphorylation, which masks a nuclear export signal within the oligomerization domain (Chène, 2001; Liang & Clarke, 2001). Additionally, Liang & Clarke provided a link between both phosphorylation sites by claiming that the formation of tetramers by serine 392 phosphorylation is reversed by serine 315 phosphorylation (Liang & Clarke, 2001).

Hence, the confluence dependent decrease in Serine 315 phosphorylation **(Figure 7.G)** combined with the inconsistent serine 392 expression found in A2780 **(Figure 7.I)** suggests masking of the nuclear localization signal at higher confluency levels and an unmasked nuclear export signal, which may lead to the transport of p53 from the nucleus to the cytoplasm. Since p53 is degraded in the cytoplasm, this further supports our previous hypothesis that increasing confluency levels may promote degradation of p53 in the cytoplasm in A2780 cells. Additionally, taking into consideration the lack of a confluence dependent change in nuclear p53 **(Figure *6*.G)**, these results suggest efficient shuttling of p53 from nucleus to cytoplasm and a confluence dependent degradation of p53 in the cytoplasm in A2780 cells.

On the other hand, the lack of consistent serine 315 expression in CP16 **(Figure 7.H)** combined with a confluence dependent increase in serine 392 **(Figure 7.J)** suggests an ineffective regulation of the nuclear localization signal and the masking of the nuclear export signal. These modifications in p53 would be expected to increase tetramerization of p53 and increase its intranuclear concentration. However, rather than an increase in nuclear p53, we observed a confluence dependent increase in cytoplasmic p53 in CP16 cells **(Figure 6.H)**. Based on these results, it can be hypothesized that the p53 mutation observed in CP16 cells which is known to prevent binding of p53 to DNA (Bhatt et al., 2017) may also disturb tetramerization of the p53 hence facilitating its transport to the cytoplasm. This may also explain why nuclear p53 does not increase significantly with confluence in CP16 cells **(Figure 6.H)**, despite its stability is increased through phosphorylation of the p53 at serine 15 **(Figure *7*.D)**.However, these hypothesis should be tested in further studies.

Upon observing a confluence dependent pattern of p53 expression on the protein level, we further investigated whether a similar pattern was also observed on the mRNA level **(Figure 8.A,B)**. Additionally, we also investigated the mRNA expression of ATM and ATR as they are mainly responsible for phosphorylating p53 at serine 15 and serine 20 (**Figure 9.A,B)**. However, our results did not reveal a confluence dependent pattern which indicates that regulation on the protein level is

responsible for the confluence dependent response to cisplatin in ovarian cancer cells, rather than changes in the gene expression.

4.2 *The role of p21 localization and phosphorylation in the confluence dependent response to cisplatin*

To further investigate which functions p53 may be inducing, we examined the expression of p21 and its subcellular localization **(Figure 10. A,B)**.

Studies have shown that nuclear p21 is capable of inducing a number of functions including, p53 dependent cell cycle arrest or p53 dependent and independent DNA repair (Karimian et al., 2016). On the other hand, many contradictions exist regarding the function of cytoplasmic p21. Research has shown that cytoplasmic p21 is associated with p21 phosphorylation sites threonine-145 and serine-146. While in some studies phosphorylated p21 was either degraded or didn't contribute to tumorigenesis, in other studies phosphorylation at these has promoted anti-apoptosis and tumorigenesis (Al Bitar & Gali-Muhtasib, 2019; Y.-S. Jung et al., 2010)

Our western blot data revealed an overall confluence dependent increase in p21 expression in both cell lines **(Figure 10.C,D)**, especially in A2780 cells. Although a statistically significant confluence dependent change in cytoplasmic p21 and nuclear p21 could not be observed due to high variance between biological replicates, cytoplasmic p21 expression seem to contribute more to the confluence dependent increase in p21 in whole cell lysates, especially in A2780 cells. Consistent with these findings, phosphorylation of p21 at threonine-145 and serine-146 exhibited a confluence dependent increase in both cell lines but more prominently in A2780 cells, despite being statistically insignificant due to high variability in biological replicates. Nuclear p21 expression in A2780 cells also showed an increasing pattern with increasing confluence yet statistically insignificant. Therefore, a clear interpretation on the role of cytoplasmic or nuclear p21 in density dependent cisplatin resistance could not be made with the present data.

4.3 *The impact of confluence level and cisplatin on apoptotic response*

To understand whether confluence dependent changes in p53 and p21 reflect to phenotypic responses they regulate, we investigated the confluence dependent changes in DNA damage marker ɣ-H2AX and several apoptosis markers **(Figure *13*.A,B)**.

We observed only a substantial but insignificant increase in ɣ-H2AX with increasing confluence in A2780 cells **(Figure *13*.C)**. However, ɣ-H2AX exhibited a significant confluence dependent increase in CP16 cells even in untreated control groups **(Figure *13*.D)**. Cisplatin treatment did not add into this increase in ɣ-H2AX in CP16 cells. These results suggested that cisplatin cannot induce DNA damage in CP16 cells, but DNA damage is highly dependent on increased cell density in this cell model. This relation is very interesting and necessitates further investigations to delineate possible mechanisms in future studies. Another surprising fact is that increasing confluence led to increased cisplatin resistance **(Figure 5.B)** despite an accompanying increase in DNA damage **(Figure *13*.D)** and a confluence dependent increase in especially cytoplasmic p53 **(Figure 6.F)** in CP16 cells.

Cytoplasmic p53 is known to interact with members of the Bcl-2 family in the mitochondria, inducing cleavage and activation of caspase-9 and caspase-3 to promote apoptosis (Hernandez Borrero & El-Deiry, 2021). In the light of these knowledge, our results suggested that there is an insensitivity to cisplatin induced DNA damage CP16 cells, which may result from a lack of apoptosis induction by p53 despite the presence of DNA damage and high expression of p53. Therefore, next we investigated apoptosis markers which are involved in different phases of the apoptosis starting from the initiation phase to the execution phase.

In contrast to our MTT results, western blot analysis in A2780 indicated increased apoptosis at higher confluency levels as both full length and cleaved forms of caspase-3 and caspase-9 increased in these groups **(Figure *13*. E,G,L,N).** This also aligns with the confluence dependent decrease in the phosphorylation of p53 at

Serine 315 (**Figure 7.G)**, since phosphorylation of this site plays a role in inhibition of mitochondrial apoptosis. These results may also explain why density dependent cisplatin resistance is very slight in A2780 cells.

On the other hand, CP16 exhibited inconsistent regulation of the full-length **(Figure *13*.F)** and cleaved form of caspase-9 **(Figure *13*.H)**. A possible explanation for this event may be sourced from the study done by Chee et al. Their research claims that the active form of caspase-9 may be inhibited by mutant cytoplasmic p53 which promotes cisplatin resistance in ovarian cancer patients (Chee et al., 2013). This may explain why caspase-9 could not be activated in CP16 cells despite increasing DNA damage with increasing cell density. Despite that, upon analysis of cleaved caspase-3 in CP16 we still observed a confluence dependent increase in expression, however this increase was not statistically significant due to high variability in biological replicates **(Figure *13*O)**. An interesting observation however is seen in the expression of full-length caspase-3 in response to cisplatin which decreased in a confluence dependent manner **(Figure *13*.M).** This may suggest that the observed cleaved caspase-3 levels are a result of the cleavage of baseline caspase-3 levels and further production of caspase-3 is reduced to prevent apoptosis in CP16 cells.

As a result of the dysregulation of mitochondrial apoptosis observed in CP16, we wondered whether p53 was mediating cell death through the extrinsic pathway instead. In this form of cell death, the initial caspase responder is caspase-8 instead of caspase-9. However, similarly to intrinsic apoptosis caspase-3 acts downstream as the final apoptotic executioner (Hernandez Borrero & El-Deiry, 2021).

In A2780, the expression of both full-length **(Figure *13*.I)** and cleaved forms of caspase-8 **(Figure *13*.K)** was inconsistent, indicating that mitochondrial apoptosis may be the dominant form of confluence dependent cell death in A2780, rather than extrinsic apoptosis. In the case of CP16, while full-length form of caspase-8 **(Figure *13*.J)** increased in expression at higher confluency levels, the expression of its cleaved form was inconsistent indicating non-functional extrinsic apoptosis.

Although the expression of caspases is one of the main indicators of apoptosis, as observed in CP16, a block in the execution of apoptosis could explain resistance (Ghavami et al., 2009) . Therefore, we investigated the expression of nuclear protein, Lamin B1, which is cleaved in response to apoptosis downstream of cleaved caspase 3. Aligning with our previous findings, cleaved Lamin B1 expressed a confluence dependent increase in A2780 **(Figure *14*.C)**, indicating higher apoptosis at overconfluent levels. However, CP16 did not display any Lamin B1 cleavage **(Figure *14*.B),** which implies that apoptosis is not taking place.

Altogether our data suggests that apoptosis induction is intact in A2780 cells which prevent a high correlation between cell density and cisplatin resistance. On the other hand, CP16 cells exhibit resistance to apoptosis despite increasing levels of DNA damage and cytoplasmic p53 with increasing cell density. Lack of apoptosis despite treatment with a cytotoxic dose of cisplatin was also interesting in CP16 cells. We propose the possibility that cell death may be occurring through other mechanisms such as necrosis or autophagy. Another possibility could be that CP16 may delay cell death, therefore our experimental design of 24 hours cisplatin treatment may not be enough to assess apoptosis. However, further investigation is required to prove these hypotheses.

4.4 *The differential expression of copper transporters in response to confluence and cisplatin.*

The ability of CP16 to regulate molecular components in a confluence dependent manner intrigued us to investigate whether other forms of chemoresistance may be regulated similarly. Therefore, we investigated the confluence dependent expression of copper transporters in response to cisplatin.

Despite CTR1 and CTR2 belonging to the same family, studies have shown that increased mRNA expression of CTR1 is associated with higher cisplatin uptake while higher levels CTR2 were associated with poor prognosis and lower survival (Lee et al., 2011). Moreover, ATP7A and ATP7B efflux pumps typically associated with

cisplatin resistance, may also be regulated through cell-cell interactions (Wilczyński et al., 2024). While neither CP16 nor A2780 showed the expected confluence dependent pattern of CTR1 expression, minimal expression at the overconfluent group in A2780 supports resistance through reduced cisplatin uptake **(Figure 16.A,B)**. However, the reasoning behind minimal expression of CTR1 at the full confluence group is unclear. Moreover, despite the presence of numerous evidence on the role of CTR2 in cisplatin transport, its inconsistent expression in both cell lines **(Figure 16,D)** may indicate that its regulation may be occurring at the protein level. Furthermore, in regards to cisplatin efflux, expression patterns of ATP7A and ATP7B do not support cisplatin resistance at the overconfluent group **(Figure 16.E,F,G,H)**. Overall, regulation of cisplatin transporters does not seem to be regulated in confluence dependent manner at the mRNA level. However, the possibility that they may be regulated by cell density at the protein level should be addressed in future studies.

4.5 *Conclusion*

This study demonstrates that confluence significantly influences cisplatin response in ovarian cancer cells, possibly through differential regulation of p53 and its downstream targets. While both A2780 and CP16 exhibited a confluence dependent increase in cisplatin IC50 values, the effect was more pronounced in CP16 **(Figure 5.C)**. Investigation of the subcellular localization and phosphorylation patterns of p53 revealed opposing patterns in both cell lines.

In A2780, a confluence dependent decrease in total and cytoplasmic p53 expression (**Figure *6*.C,E)** was observed without corresponding changes in nuclear p53 (**Figure 6.G)**, suggesting enhanced degradation of p53 in the cytoplasm. This further was supported by the reduced expression of serine 15 and serine 20 at higher confluence groups **(Figure 7.C,E)**, suggesting a reduction in p53 stability. Meanwhile, the combined confluence dependent decrease in serine 315 and inconsistent serine 392 expression **(Figure 7.G,I)** pointed towards downregulation of nuclear import and possible upregulation of nuclear export of p53.Conversely, the confluence dependent increase in total and cytoplasmic p53 in CP16 **(Figure 6.D,F)** alongside elevated

serine 15 and serine 20 expression **(Figure 7. D,F)** indicate cytoplasmic accumulation of p53 due to increased stability. Investigation of p53's downstream target p21 revealed a confluence dependent increase in total levels in both cell lines **(Figure 10.C,D)**. However, only A2780 displayed a consistent and confluence dependent decrease in nuclear p21 **(Figure 10.G)** pointing towards effective regulation of cell cycle arrest in the A2780 but not in CP16.

Finally, We observed an intact apoptotic response to cisplatin A2780 cells which may explain a slight change in resistance with increasing confluence. However, we observed an impairment in the execution of apoptosis in CP16 cells **(Figure 14.B) (Figure 15)**, which may explain why these cells exhibit a prominent density dependent resistance to cisplatin despite an interesting increase in DNA damage **(Figure *13*.D)** and cytoplasmic p53 expression with increasing cellular density in these cells **(Figure 6.F)**. P53 mutation in these cells may be a possible explanation to this response. To validate that we are planning to perform CRISPR inactivation of mutant p53 and overexpression of wild type p53 in future studies. These knock-down and overexpression studies are also essential to validate the role of p53 in density dependent cisplatin resistance, since simultaneous changes in some molecules and cellular responses do not necessarily indicate a causal relationship.

Besides intracellular signaling aspect presented in this study, how cancer cells communicate with each other to exhibit an emergent behavior (density dependent cisplatin resistance in our case) warrants delineation. In future studies we are planning to investigate how cell-cell contact and paracrine signaling may modulate mechanism of action of cisplatin and mechanisms of resistance to cisplatin in ovarian cancer cells. Moreover, signaling mechanisms that induce cell survival and proliferation such as PI3K/Akt, MAPK pathways may also play key roles in density-dependent cisplatin resistance in ovarian cancer, which we will address in prospective studies. These studies can shed further light into the mechanisms of density dependent cisplatin resistance in ovarian cancer.

BIBLIOGRAPHY

Abbas, T., & Dutta, A. (2009). p21 in cancer: intricate networks and multiple activities. *Nat Rev Cancer*, *9*(6), 400-414. https://doi.org/10.1038/nrc2657

Al Bitar, S., & Gali-Muhtasib, H. (2019). The Role of the Cyclin Dependent Kinase Inhibitor p21cip1/waf1 in Targeting Cancer: Molecular Mechanisms and Novel Therapeutics. *Cancers*, *11*(10), 1475. https://www.mdpi.com/2072-6694/11/10/1475

Ali, R., Aouida, M., Alhaj Sulaiman, A., Madhusudan, S., & Ramotar, D. (2022). Can Cisplatin Therapy Be Improved? Pathways That Can Be Targeted. *Int J Mol Sci*, *23*(13). https://doi.org/10.3390/ijms23137241

Bhatt, M., Ivan, C., Xie, X., & Siddik, Z. H. (2017). Drug-dependent functionalization of wild-type and mutant p53 in cisplatin-resistant human ovarian tumor cells. *Oncotarget*, *8*(7), 10905-10918. https://doi.org/10.18632/oncotarget.14228

Blaydes, J. P., Luciani, M. G., Pospisilova, S., Ball, H. M.-L., Vojtesek, B., & Hupp, T. R. (2001). Stoichiometric Phosphorylation of Human p53 at Ser³¹⁵Stimulates p53-dependent Transcription *. *Journal of Biological Chemistry*, *276*(7), 4699-4708. https://doi.org/10.1074/jbc.M003485200

Chee, J. L., Saidin, S., Lane, D. P., Leong, S. M., Noll, J. E., Neilsen, P. M., Phua, Y. T., Gabra, H., & Lim, T. M. (2013). Wild-type and mutant p53 mediate cisplatin resistance through interaction and inhibition of active caspase-9. *Cell Cycle*, *12*(2), 278-288. https://doi.org/10.4161/cc.23054

Chen, S. H., & Chang, J. Y. (2019). New Insights into Mechanisms of Cisplatin Resistance: From Tumor Cell to Microenvironment. *Int J Mol Sci*, *20*(17). https://doi.org/10.3390/ijms20174136

Chène, P. (2001). The role of tetramerization in p53 function. *Oncogene*, *20*(21), 2611-2617. https://doi.org/10.1038/sj.onc.1204373

Cheng, C. W., & Tse, E. (2018). PIN1 in Cell Cycle Control and Cancer. *Front Pharmacol*, *9*, 1367. https://doi.org/10.3389/fphar.2018.01367

Cmielova, J., & Rezacova, M. (2011). p21Cip1/Waf1 protein and its function based on a subcellular localization [corrected]. *J Cell Biochem*, *112*(12), 3502-3506. https://doi.org/10.1002/jcb.23296

Coalition, W. O. C. (2023). *The World Ovarian Cancer Coalition 2023*. Retrieved 30.10.2024 from https://worldovariancancercoalition.org/wp-content/uploads/2023/04/World-Ovarian-Cancer-Coalition-Atlas-2023-FINAL.pdf

Dasari, S., & Tchounwou, P. B. (2014). Cisplatin in cancer therapy: molecular mechanisms of action. *Eur J Pharmacol*, *740*, 364-378. https://doi.org/10.1016/j.ejphar.2014.07.025

Dyson, H. J., & Wright, P. E. (2025). How does p53 work? Regulation by the intrinsically disordered domains. *Trends in Biochemical Sciences*, *50*(1), 9-17. https://doi.org/10.1016/j.tibs.2024.10.009

ESMO, E. S. f. M. O. (2017). *ESMO Patient Guide Series* Retrieved 30.10.24 from https://www.esmo.org/content/download/10097/201883/1/EN-Ovarian-Cancer-Guide-for-Patients.pdf

Facchin, S., Ruzzene, M., Peggion, C., Sartori, G., Carignani, G., Marin, O., Brustolon, F., Lopreiato, R., & Pinna, L. A. (2007). Phosphorylation and activation of the atypical kinase p53-related protein kinase (PRPK) by Akt/PKB. *Cellular and Molecular Life Sciences*, *64*(19), 2680. https://doi.org/10.1007/s00018-007-7179-7

Friedrich Marks, U. K., Karin Müller-Decker. (2017). *Cellular Signal Processing An Introduction to the Molecular Mechanisms of Signal Transduction* (Second ed.). Garland Science.

Galluzzi, L., Vitale, I., Aaronson, S. A., Abrams, J. M., Adam, D., Agostinis, P., Alnemri, E. S., Altucci, L., Amelio, I., Andrews, D. W., Annicchiarico-Petruzzelli, M., Antonov, A. V., Arama, E., Baehrecke, E. H., Barlev, N. A., Bazan, N. G., Bernassola, F., Bertrand, M. J. M., Bianchi, K., . . . Kroemer, G. (2018). Molecular mechanisms of cell death: recommendations of the Nomenclature Committee on Cell Death 2018. *Cell Death & Differentiation*, *25*(3), 486-541. https://doi.org/10.1038/s41418-017-0012-4

Ghavami, S., Hashemi, M., Ande, S. R., Yeganeh, B., Xiao, W., Eshraghi, M., Bus, C. J., Kadkhoda, K., Wiechec, E., Halayko, A. J., & Los, M. (2009). Apoptosis and cancer: mutations within caspase genes. *Journal of Medical Genetics*, *46*(8), 497-510. https://doi.org/10.1136/jmg.2009.066944

Ghosh, S. (2019). Cisplatin: The first metal based anticancer drug. *Bioorganic Chemistry*, *88*, 102925. https://doi.org/https://doi.org/10.1016/j.bioorg.2019.102925

Green, D. R., & Kroemer, G. (2009). Cytoplasmic functions of the tumour suppressor p53. *Nature*, *458*(7242), 1127-1130. https://doi.org/10.1038/nature07986

Hafner, A., Bulyk, M. L., Jambhekar, A., & Lahav, G. (2019). The multiple mechanisms that regulate p53 activity and cell fate. *Nature Reviews Molecular Cell Biology*, *20*(4), 199-210. https://doi.org/10.1038/s41580-019-0110-x

He, Y., Zhu, Q., Chen, M., Huang, Q., Wang, W., Li, Q., Huang, Y., & Di, W. (2016). The changing 50% inhibitory concentration (IC50) of cisplatin: a pilot study on the artifacts of the MTT assay and the precise measurement of density-dependent chemoresistance in ovarian cancer. *Oncotarget*, *7*(43), 70803-70821. https://doi.org/10.18632/oncotarget.12223

Hernandez Borrero, L. J., & El-Deiry, W. S. (2021). Tumor suppressor p53: Biology, signaling pathways, and therapeutic targeting. *Biochim Biophys Acta Rev Cancer*, *1876*(1), 188556. https://doi.org/10.1016/j.bbcan.2021.188556

Jack, M. T., Woo, R. A., Motoyama, N., Takai, H., & Lee, P. W. K. (2004). DNA-dependent Protein Kinase and Checkpoint Kinase 2 Synergistically Activate a Latent Population of p53 upon DNA Damage*. *Journal of Biological Chemistry*, *279*(15), 15269-15273. https://doi.org/https://doi.org/10.1074/jbc.M309917200

Jung, Y.-S., Qian, Y., & Chen, X. (2010). Examination of the expanding pathways for the regulation of p21 expression and activity. *Cellular Signalling*, *22*(7), 1003-1012. https://doi.org/https://doi.org/10.1016/j.cellsig.2010.01.013

Jung, Y. S., Qian, Y., & Chen, X. (2010). Examination of the expanding pathways for the regulation of p21 expression and activity. *Cell Signal*, *22*(7), 1003-1012. https://doi.org/10.1016/j.cellsig.2010.01.013

Kapoor, M., Hamm, R., Yan, W., Taya, Y., & Lozano, G. (2000). Cooperative phosphorylation at multiple sites is required to activate p53 in response to UV radiation. *Oncogene*, *19*(3), 358-364. https://doi.org/10.1038/sj.onc.1203300

Karimian, A., Ahmadi, Y., & Yousefi, B. (2016). Multiple functions of p21 in cell cycle, apoptosis and transcriptional regulation after DNA damage. *DNA Repair (Amst)*, *42*, 63-71. https://doi.org/10.1016/j.dnarep.2016.04.008

Lee, Y.-Y., Choi, C. H., Do, I.-G., Song, S. Y., Lee, W., Park, H. S., Song, T. J., Kim, M. K., Kim, T.-J., Lee, J.-W., Bae, D.-S., & Kim, B.-G. (2011). Prognostic value of the copper transporters, CTR1 and CTR2, in patients with ovarian carcinoma receiving platinum-based chemotherapy. *Gynecologic Oncology*, *122*(2), 361-365. https://doi.org/https://doi.org/10.1016/j.ygyno.2011.04.025

Liang, S.-H., & Clarke, M. F. (2001). Regulation of p53 localization. *European Journal of Biochemistry*, *268*(10), 2779-2783. https://doi.org/https://doi.org/10.1046/j.1432-1327.2001.02227.x

Lu, H., Fisher, R. P., Bailey, P., & Levine, A. J. (1997). The CDK7-cycH-p36 Complex of Transcription Factor IIH Phosphorylates p53, Enhancing Its Sequence-Specific DNA Binding Activity In Vitro. *Molecular and Cellular Biology*, *17*(10), 5923-5934. https://doi.org/10.1128/MCB.17.10.5923

Lukanović, D., Herzog, M., Kobal, B., & Černe, K. (2020). The contribution of copper efflux transporters ATP7A and ATP7B to chemoresistance and personalized medicine in ovarian cancer. *Biomed Pharmacother*, *129*, 110401. https://doi.org/10.1016/j.biopha.2020.110401

Makovec, T. (2019). Cisplatin and beyond: molecular mechanisms of action and drug resistance development in cancer chemotherapy. *Radiol Oncol*, *53*(2), 148-158. https://doi.org/10.2478/raon-2019-0018

Marei, H. E., Althani, A., Afifi, N., Hasan, A., Caceci, T., Pozzoli, G., Morrione, A., Giordano, A., & Cenciarelli, C. (2021). p53 signaling in cancer progression and therapy. *Cancer Cell Int*, *21*(1), 703. https://doi.org/10.1186/s12935-021-02396-8

Meek, D. W. (2013). The Role of Protein Kinase CK2 in the p53 Response. In *Protein Kinase CK2* (pp. 190-204). https://doi.org/https://doi.org/10.1002/9781118482490.ch6

Mitsuuchi, Y., Johnson, S. W., Selvakumaran, M., Williams, S. J., Hamilton, T. C., & Testa, J. R. (2000). The phosphatidylinositol 3-kinase/AKT signal transduction pathway plays a critical role in the expression of p21WAF1/CIP1/SDI1 induced by cisplatin and paclitaxel. *Cancer Res*, *60*(19), 5390-5394.

Nantajit, D., Fan, M., Duru, N., Wen, Y., Reed, J. C., & Li, J. J. (2010). Cyclin B1/Cdk1 Phosphorylation of Mitochondrial p53 Induces Anti-Apoptotic

Response. *PLOS ONE*, *5*(8), e12341. https://doi.org/10.1371/journal.pone.0012341

O'Brate, A., & Giannakakou, P. (2003). The importance of p53 location: nuclear or cytoplasmic zip code? *Drug Resistance Updates*, *6*(6), 313-322. https://doi.org/https://doi.org/10.1016/j.drup.2003.10.004

Öhrvik, H., & Thiele, D. J. (2015). The role of Ctr1 and Ctr2 in mammalian copper homeostasis and platinum-based chemotherapy. *J Trace Elem Med Biol*, *31*, 178-182. https://doi.org/10.1016/j.jtemb.2014.03.006

POSPÍŠILOVÁ, Š., BRÁZDA, V., KUCHAŘÍKOVÁ, K., LUCIANI, M. G., HUPP, T. R., SKLÁDAL, P., PALEČEK, E., & VOJTĚŠEK, B. (2004). Activation of the DNA-binding ability of latent p53 protein by protein kinase C is abolished by protein kinase CK2. *Biochemical Journal*, *378*(3), 939-947. https://doi.org/10.1042/bj20030662

Punyamurtula, U., Brown, T. W., Zhang, S., George, A., & El-Deiry, W. S. (2023). Cancer cell seeding density as a mechanism of chemotherapy resistance: a novel cancer cell density index based on IC50-Seeding Density Slope (ISDS) to assess chemosensitivity. *Am J Cancer Res*, *13*(12), 5914-5933.

Radhakrishnan, S. K., & Gartel, A. L. (2006). CDK9 phosphorylates p53 on serine residues 33, 315 and 392. *Cell Cycle*, *5*(5), 519-521. https://doi.org/10.4161/cc.5.5.2514

Schoeberl, A., Gutmann, M., Theiner, S., Corte-Rodriguez, M., Braun, G., Vician, P., Berger, W., & Koellensperger, G. (2022). The copper transporter CTR1 and cisplatin accumulation at the single-cell level by LA-ICP-TOFMS. *Front Mol Biosci*, *9*, 1055356. https://doi.org/10.3389/fmolb.2022.1055356

Schoeberl, A., Gutmann, M., Theiner, S., Corte-Rodríguez, M., Braun, G., Vician, P., Berger, W., & Koellensperger, G. (2022). The copper transporter CTR1 and cisplatin accumulation at the single-cell level by LA-ICP-TOFMS [Original Research]. *Frontiers in Molecular Biosciences*, *Volume 9 - 2022*. https://doi.org/10.3389/fmolb.2022.1055356

Siddik, Z. H. (2003). Cisplatin: mode of cytotoxic action and molecular basis of resistance. *Oncogene*, *22*(47), 7265-7279. https://doi.org/10.1038/sj.onc.1206933

Smith, H. L., Southgate, H., Tweddle, D. A., & Curtin, N. J. (2020). DNA damage checkpoint kinases in cancer. *Expert Rev Mol Med*, *22*, e2. https://doi.org/10.1017/erm.2020.3

Wilczyński, B., Dąbrowska, A., Kulbacka, J., & Baczyńska, D. (2024). Chemoresistance and the tumor microenvironment: the critical role of cell–cell communication. *Cell Communication and Signaling*, *22*(1), 486. https://doi.org/10.1186/s12964-024-01857-7